Science of the Total Environment 892 (2023) 164754

Contents lists available at ScienceDirect

Science of the Total Environment

journal homepage: www.elsevier.com/locate/scitotenv

Investigation of simultaneous effects of noise barriers on near-road noise and air pollutants

Melike Nese Tezel-Oguz [a,b,*], Muhammed Marasli [c], Deniz Sari [a], Nesimi Ozkurt [a], S. Sinan Keskin [b]

[a] TUBITAK Marmara Research Center, Vice Presidency of Climate Change and Sustainability, 41470 Kocaeli, Turkey
[b] Marmara University, Department of Environmental Engineering, 34854 Istanbul, Turkey
[c] Fibrobeton Inc., Istanbul 34810, Turkey

HIGHLIGHTS

- Studies show that noise barriers can help to reduce air pollutant concentrations.
- Measurements were performed at the road and receptor sides of a noise barrier.
- The barrier reduced average NO_x levels by 23 % besides the noise level reduction.
- The noise and air pollution models produced compatible results to measurements.
- The dispersion mechanisms of noise and air pollution near a barrier are different.

ARTICLE INFO

Editor: Pavlos Kassomenos

Keywords:
Noise barrier
Road-traffic noise
Near-road air pollution
Combined exposure

ABSTRACT

Noise barriers are one of the common solutions to control road traffic noise. Many studies have also shown that noise barriers cause reductions in near-road air pollutant concentrations. In this study, the simultaneous effects of a specific noise barrier application on near-road noise and air pollution at a specific location were investigated. In this context, air pollution, noise, and meteorological parameters were measured simultaneously at two points, road and receptor sides of a 50 m long, 4 m high glass fiber reinforced concrete noise barrier on a highway section. Results indicated that the noise barrier has an average 23 % reduction effect on the NO_x concentration in addition to the noise level reduction at the receptor side. Besides, bi-weekly average passive sampler measurement results for BTEX pollutants indicate lower values at the receptor side of the barrier compared to the free field measurement results. In addition to real-time and passive sampler measurements, NO_x and noise dispersions were modeled using RLINE and SoundPLAN 8.2 software, respectively. Comparisons of the measurement results with the model results indicated strong correlations. Model-calculated NO_x and noise values under the free field conditions are highly compatible with a correlation coefficient (r) of 0.78. Although the noise barrier has a reduction effect on both parameters, it has been observed that their dispersion mechanisms are different. This study showed that noise barriers considerably affect the dispersion of road-sourced air pollutants at the receptor side. Further studies are needed to optimize noise barrier designs with different physical and material properties and application scenarios considering noise and air pollutants together.

1. Introduction

In today's urban life, noise has become one of the most important factors negatively affecting human health due to not considering environmental noise in urban planning strategies (Zannin et al., 2018). Noise emission is one of the significant environmental issues that should be handled with high priority in a heavily populated area (Shahidan et al., 2017). Although noise is an output of many human activities, environmental noise sources related to transportation are the most prevalent. After airborne fine particulate matter pollution, transport-related noise is regarded as having Europe's second-largest environmental impact on human health. Therefore, environmental noise, particularly road traffic, is a significant environmental issue in Europe. In the EU, prolonged day-evening-night traffic noise levels of at least 55 dBA impact about 113 million individuals (EEA, 2020). Many epidemiological studies have associated noise exposure with cardiovascular conditions, high blood pressure, sleep disorders, and cognitive impairment (Basner et al., 2014; Cassina et al., 2018; Lercher et al., 2003; Miedema and Oudshoorn, 2001; Ross et al., 2011; Sygna et al., 2014). Determination, elimination, and avoidance of environmental noise were targeted with directives and regulations to prevent or reduce harmful

* Corresponding author at: TUBITAK Marmara Research Center, Vice Presidency of Climate Change and Sustainability, 41470 Kocaeli, Turkey.
E-mail address: nese.tezel@tubitak.gov.tr (M.N. Tezel-Oguz).

http://dx.doi.org/10.1016/j.scitotenv.2023.164754
Received 6 May 2023; Received in revised form 28 May 2023; Accepted 6 June 2023
Available online 10 June 2023

effects of environmental noise (END, 2002; MoEUCC, 2022). Milford et al. (2012) investigated the most beneficial noise abatement strategies among noise barriers, façade insulation, quieter road surfaces, and quieter vehicles regarding annoyance and cost-effectiveness. They stated that noise reduction at the source is the most cost-effective approach to reducing noise annoyance (Milford et al., 2012). Due to inefficient planning and lack of access to other, more efficient methods, noise barriers became a common noise abatement measure, especially for vehicle noise.

A research study by the Health Effects Institute showed that specific adverse health effects, such as diminished lung capacity and cardiovascular mortality, are associated with staying within approximately 300–500 m of the main road (HEI, 2010). In the United States, 75 % of carbon monoxide was emitted from mobile sources in 2008. According to a past EPA study, over 100 million people were exposed to road-traffic noise levels that may be harmful to health (Cooper and Alley, 2011). Motor vehicle exhaust gases have a particularly negative impact on enclosed areas near busy roads. Air pollution has been linked to cardiovascular diseases, hypertension, and atherosclerosis and is a significant global risk factor for premature morbidity and mortality (Brook et al., 2010; Foraster et al., 2011; Fuks et al., 2017; Rao et al., 2014). Several in-situ studies (Baldauf et al., 2008; Finn et al., 2010; Hagler et al., 2012; Hooghwerff et al., 2010; Lee et al., 2018; Ning et al., 2010; Ranasinghe et al., 2019; Thiruvenkatachari et al., 2022) and wind tunnel studies (Heist et al., 2009; Kanda et al., 2011) have indicated that noise barriers can also reduce the near-road air pollutants emitted by vehicles besides noise. In addition to measurements, several modeling studies have been performed to assess the effects of noise barriers on air pollutant dispersion (Adair and Jaeger, 2014; Ahangar et al., 2017; Amini et al., 2018; Ghasemian et al., 2017; Gong and Wang, 2018; Hagler et al., 2011; Heist et al., 2013; Huertas et al., 2021; Jeong, 2015; Morakinyo and Lam, 2016; Reiminger et al., 2020; Schulte et al., 2014; Steffens et al., 2014; Steffens et al., 2013; Steffens et al., 2012; Tong et al., 2016; Venkatram et al., 2021; Venkatram et al., 2016; Wang and Wang, 2021). Noise barriers can influence air pollutants' dispersion by increasing vertical mixing due to the structure-induced upward airflow deflection. Studies indicate that this upward air deflection can create a recirculation cavity downwind of the barrier, extending downwind from 3 to 12 wall heights, containing a well-mixed and often lower concentration zone of pollution (Baldauf et al., 2008).

Shu et al. (2014) found a moderate correlation between L_{eqA} and ultrafine particles (UFP) under downwind conditions and observed that a noise barrier altered the linear relationship between L_{eqA} and UFP. Although many publications have evaluated the relationship between road-traffic noise and air pollution (Danciulescu et al., 2015; Davies et al., 2009; Dekoninck and Severijnen, 2022; Foraster et al., 2011; Khan et al., 2018; Kheirbek et al., 2014; Kim et al., 2012; Ning et al., 2010; Shu et al., 2014; Tang and Wang, 2007), examining the simultaneous effect of noise barriers on the dispersion of noise and air pollutants originating from roads needs further research.

Noise simulation tools can calculate noise levels and are instrumental in planning stages. CadnA, TRANEX, and SoundPLAN have been widely used software for noise mapping (Khan et al., 2018). They are regarded as a capable, efficient, and generally accurate tool for simulating road-traffic noise (Karantonis et al., 2010). SoundPLAN was used in many previous studies to assess near-road (Ece et al., 2018; Hasmaden et al., 2022; Medeiros et al., 2022) and near-railway (Fiorini, 2022) noise barrier performances with various scenarios. Tsai et al. (2019) explored noise levels along central Taiwan's Taiwan High-Speed Rail (THSR) network through noise measurements, simulations, and questionnaire surveys. Their results showed that L_{eq} and L_{max} predicted using SoundPLAN were more precise than those predicted using CadnaA. They used the SoundPLAN 8.2 software to model noise levels originating from railway traffic and to see the effect of noise barriers on noise dispersion.

An air quality model is a mathematical representation of the mechanism that controls the fate of air pollutants released into the atmosphere. Existing models can be divided into several categories: computational fluid dynamics (CFD) models, semi-empirical box models, semi-empirical Gaussian plume models, Lagrangian particle models, and unsteady Gaussian puff models. Using different approaches to model air pollution is convenient depending on source-receptor distances. A continuously emitted pollutant within distances of tens of kilometers from the source is treated as a plume governed by meteorology near the pollutant source (Venkatram and Schulte, 2018). Heist et al. (2013) compared the capability of four different models based on the Gaussian plume diffusion equation of the steady-state, CALINE, AERMOD, ADMS-Urban, and RLINE, to simulate air pollutants concentrations near highways. Generally, RLINE, ADMS, and AERMOD (all source types) had broadly similar overall output statistics (Heist et al., 2013). Snyder et al. (2013) evaluated the RLINE model with the line source field study conducted in Idaho Falls (Finn et al., 2010). The model performed well for most meteorological conditions and slightly underpredicted the observed values. RLINE was also evaluated with near-roadway measurements taken during a tracer study in Sacramento, CA (Benson, 1992) and an actual NO emissions study in Raleigh, NC (Baldauf et al., 2008), both of which were conducted with traffic present on major freeways. In these studies, RLINE performed well for receptors downwind of the roadways, with a tendency to slightly over-predict (Snyder et al., 2013). In addition to these results, RLINE is explicitly designed for near-road applications and differs from other models with algorithms for depressed roadways and roadways with a noise barrier (Snyder et al., 2013). Moreover, several recent epidemiologic studies have used the RLINE source dispersion model to estimate traffic-related air pollutants (TRAP) exposure (Batterman et al., 2015; Pachón et al., 2016; Zhai et al., 2016).

This study examines the simultaneous effects of near-road noise barriers on noise and air pollution next to a major highway. In this context, air pollution, noise, and meteorological measurements have been performed in a road section where a glass fiber-reinforced concrete noise barrier is located at the roadside. When fossil fuel is burned at a high temperature, nitrogen oxides (NO_x), a family of highly reactive and toxic gases, are produced (USEPA, 2022). BTEX [1,2,4-trimethylbenzene, benzene, toluene, ethylbenzene, and xylene isomers (m-xylene, p-xylene, o-xylene)] is a common contaminant group that belongs to volatile organic compounds (VOCs) which are emitted from motor vehicle exhaust and other biogenic sources (Mehta et al., 2020). A robust nonlinear relationship exists between the Ozone (O_3) concentration and the emission of specific atmospheric precursors, VOCs, and NO_x (Y. Wang et al., 2018). Due to these reasons, NO, NO_2, NO_x, O_3, and BTEX concentrations together with noise levels, were measured within the same time interval in the study area. Dispersion model simulations of noise and air pollutants were conducted using the SoundPLAN 8.2 and RLINE modeling software, respectively. The consistency between the measurement and model-produced computational results was analyzed. Finally, the relationship between noise and air pollutants was examined using these models.

2. Materials and methods

2.1. Site measurements

The field study was performed in an area with an existing glass fiber-reinforced concrete noise barrier. The 50 m long and 4 m high barrier is located on one side of the D100 highway in Duzce, Turkiye. Simultaneous measurements were carried out on the road and receptor sides of the barrier to determine the dispersion of road traffic-sourced noise and air pollutants. Hourly noise, NO, NO_2, NO_x, and O_3 real-time measurements were carried out at two points, one on the roadside and the other on the receptor side of the barrier, during September 22–29, 2022. In addition, to see the cumulative effect of the dispersion of BTEX, NO_2, and O_3 concentrations, passive sampler tubes were located in the study area between September 20, 2022 and October 6, 2022 at 20 points (5 at the roadside, 12 at the receptor side of the barrier, and 3 at the free field conditions). In addition, to create a traffic emission inventory as an input to noise and air pollution simulation models, road traffic was recorded on video during the measurement period, and meteorological parameter measurements were carried out. The

measurement points and the site plan are shown in Fig. 1. Photos from the study area are given in Fig. 2.

The geographical database is the primary input for noise and air pollution dispersion models. For this reason, the region's geographical database has been created by obtaining the terrain elevations. The terrain elevation data were obtained from the Duzce Municipality's base map and "Shuttle Radar Topography Mission (SRTM) 90m Digital Elevation Data" provided by the National Aeronautics and Space Administration (NASA) of the USA (NASA, 2021). A digital ground model of the study area was created in SoundPLAN 8.2, but RLINE does not account for variations in terrain elevation as it is currently formulated as a flat-terrain model. The locations and specifications of buildings were obtained from Duzce Municipality's base map and used as input data for both SoundPLAN and RLINE models.

2.1.1. Vehicle counts

Hourly vehicle numbers are essential for both SoundPLAN and RLINE simulation models to calculate road emissions that differ according to the used standards. In SoundPLAN 8.2, the emission level may include different vehicle numbers, types or other corrections. The emission level can be calculated automatically from the input parameters. The emission changes due to a change in traffic volume, road surface, traffic speed etc. are stored at all road segments (SoundPLAN, 2019). In RLINE, emissions from a line source are characterized by an emission rate that depends on vehicle numbers and emission factors of these vehicles (Snyder et al., 2013; Venkatram and Schulte, 2018). Hourly vehicle counts in the study area were obtained through video recordings near the D100 road section during September 22–29, 2022 to create a proper input dataset for simulations. Video recordings were processed with counting analytics software to count the vehicles. Hourly vehicle numbers were obtained for the D100 road section through the software, as shown in Fig. 3.

There are four distinct periods for hourly vehicle numbers; rapid increase (06:00 to 08:00), high value (08:00 to 19:00), rapid decrease (19:00 to 02:00), and low value (02:00 to 06:00). During weekdays, vehicle numbers in these periods ranged from 300 to 1350, 1100 to 1650, 1650 to 250, and 150 to 300, respectively. During Saturday and especially Sunday, hourly vehicle numbers decreased from 06:00 to 12:00.

2.1.2. Meteorological measurements and data supply

Near-surface wind speed readings obtained from stations in suburban areas, along with related information on roughness, duration, and albedo, can be used to predict meteorological inputs for dispersion models (Venkatram and Schulte, 2018). The main inputs of the meteorological pre-processor are surface meteorological data (cloud height, wind direction, wind speed, pressure, temperature, humidity, and cloudiness) and upper-air data. Wind speed, wind direction, temperature, pressure, and humidity measurements were performed with Vaisala Weather Transmitter WXT520 during September 22–29, 2022 in field conditions when vehicle counts, noise, NO, NO_2, NO_x, and O_3 measurements were performed. The location of the meteorological measurement station is given in Fig. 1. Cloud height and cloudiness data were obtained from the Turkish State Meteorological Service's Duzce Meteorological Station. The temperature and cloudiness data for the measurement period are presented in Fig. 4. Higher cloudiness levels and lower average temperatures were observed during the first week of the field study when the real-time and passive tube measurements were performed simultaneously, compared to the second week when only the passive tube measurements continued.

Upper air meteorological data have been obtained from Kartal meteorological station in Istanbul. Surface and upper air meteorological data were processed by the AERMET pre-processor to consider the effects of meteorological conditions on pollutant dispersion. The windrose plot for the two weeks measurement period is given in Fig. 5. Since the dominant wind direction was from the south during the measurement period, the noise barrier position was in the downwind direction. Generally, low wind speeds were dominant and calm conditions (<2 m/s) were observed during the

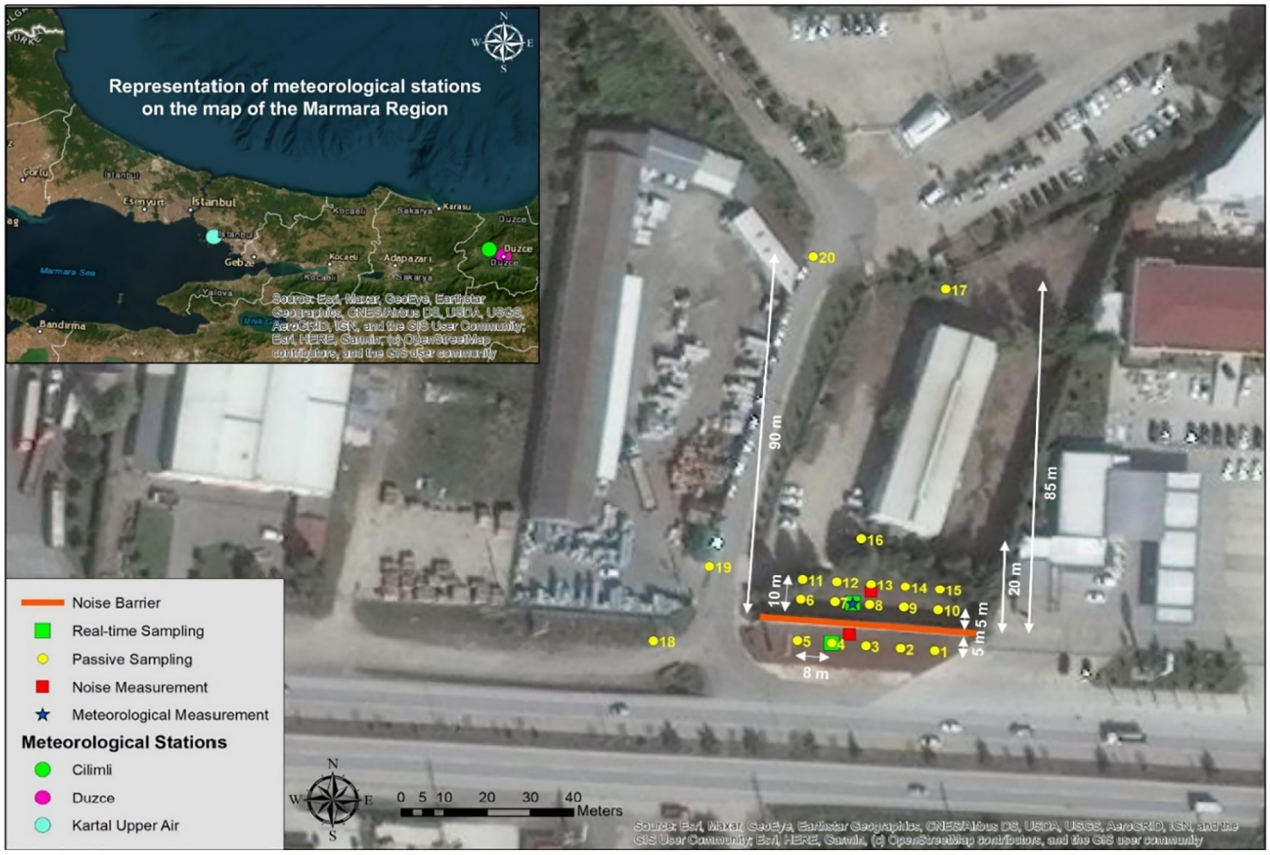

Fig. 1. Measurement points and the site plan.

(a) Road side of the barrier (b) Receptor side of the barrier

Fig. 2. Photos from the study area.

measurement period. The output data from the meteorological AERMET pre-processor were used as input to the RLINE modeling software.

In general, there are three types of sound propagation which are homogeneous propagation (sound rays are straight), favorable propagation (downward-curved sound rays cause an increase in sound level), and unfavorable propagation (upward-curved sound rays cause attenuation in sound level) (NMPB, 1996). The effect of meteorological conditions is not measurable as soon as the distance between the source and the receptor is <100 m. Moreover, due to the lack of harmonized meteorological classification scheme across Europe, conditions that are 50 % favorable and 50 % homogeneous during daytime, 75 % favorable and 25 % homogeneous during evening time, 100 % favorable and 0 % homogeneous during nighttime were used in noise modeling calculations (Kephalopoulos et al., 2014).

2.1.3. Air pollutant measurements

Two measurement points were determined at the roadside and the receptor side of the noise barrier within the study area for real-time NO, NO_2, NO_x, and O_3 concentration measurements on a 24-h basis during one-week period. Environnement S.A. Model AC32M Chemiluminescent Nitrogen Oxides Analyzers were used to measure NO, NO_2, and NO_x concentrations in ambient air at both sides of the barrier. Thermo Scientific Model 49i and Environnement S.A. Model $O_3$42M UV Photometric Ozone Analyzers were used to measure the hourly O_3 concentrations in ambient air at the road and receptor sides of the barrier, respectively. In addition to hourly real-time concentration measurements, NO_2, O_3, and BTEX passive sampler tubes were located at 20 sampling points (Fig. 1). The real-time and the passive tube measurements were performed at similar heights. With passive sampler tubes deployed at designated sampling points, air

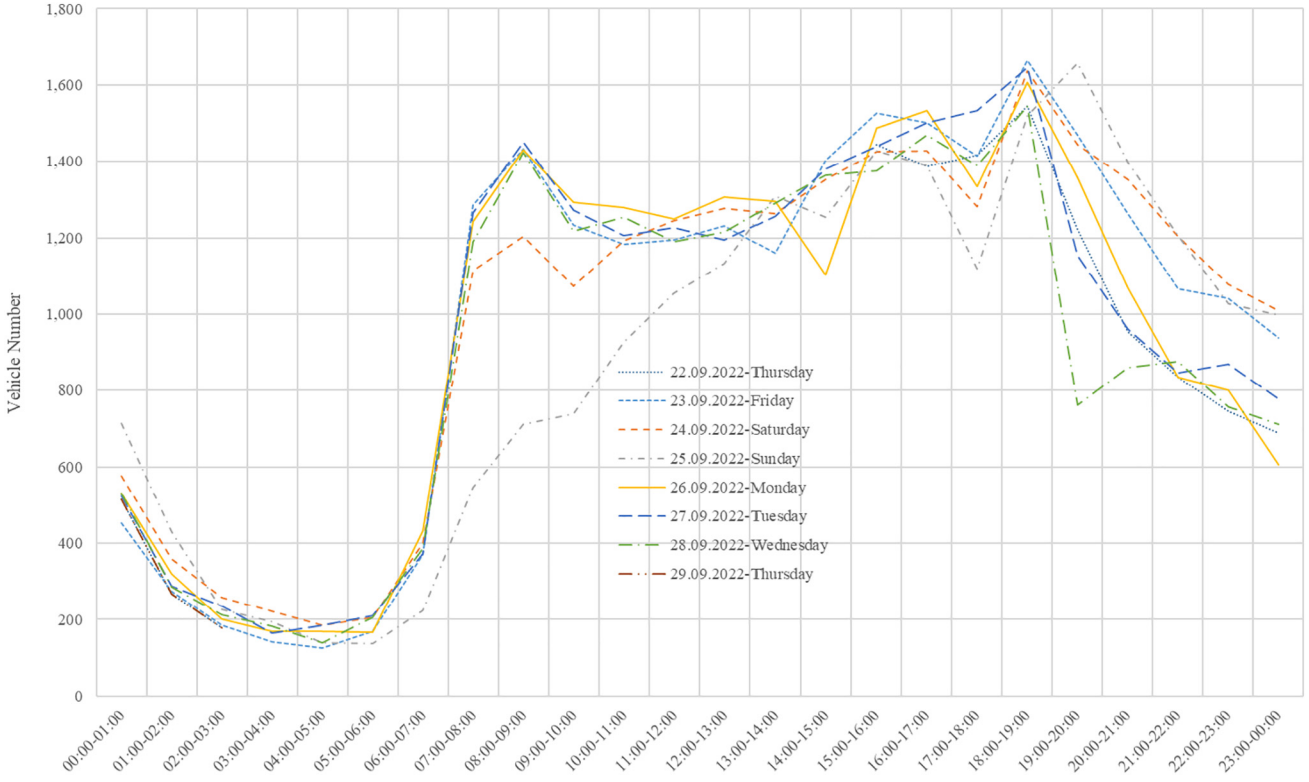

Fig. 3. Hourly vehicle counts.

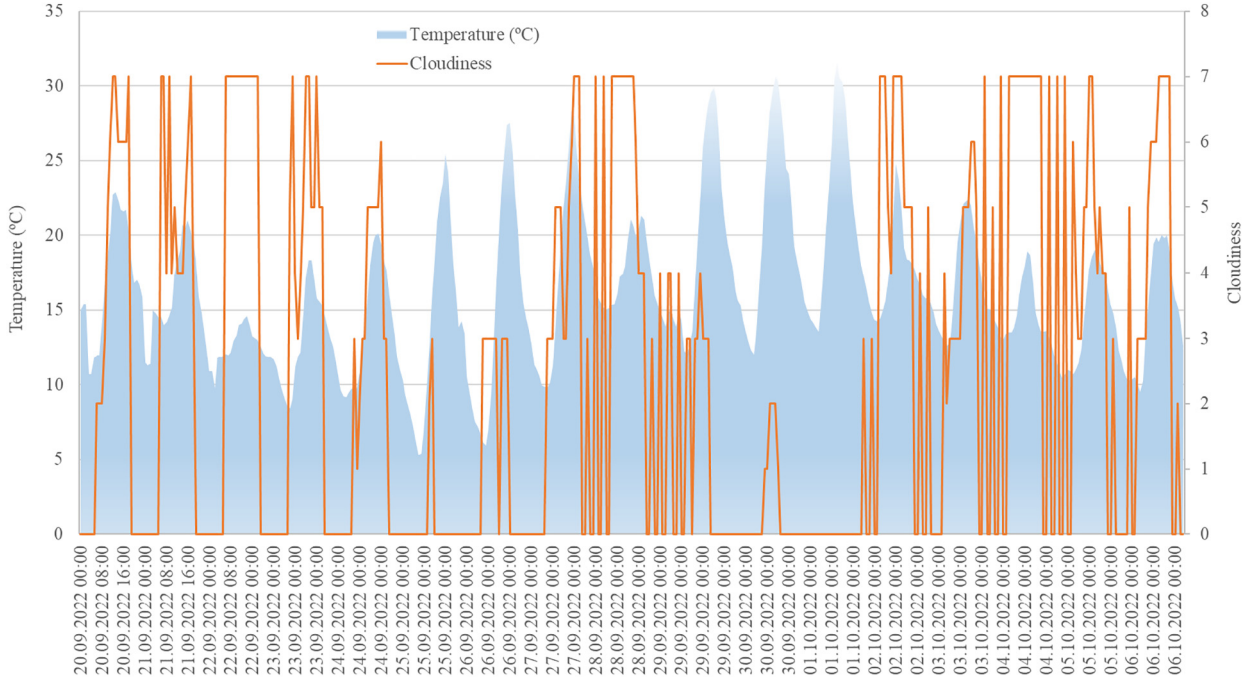

Fig. 4. Temperature and cloudiness data during the measurement period.

samples were collected from ambient air during two-weeks period (20/09/2022–06/10/2022) by absorption based on the diffusion principle. After the collection step, passive tubes were analyzed by ion chromatography for NO_2 and O_3 concentrations and gas chromatography–mass spectrometry for BTEX concentrations. Fractional expanded uncertainties of benzene, toluene, ethylbenzene, o-xylene, mp-xylene, NO_2, and O_3 are 0.13, 0.14, 0.14, 0.13, 0.13, 0.08, and 0.10, respectively.

2.1.4. Noise measurements

Noise dispersion maps are suggested to be verified by measurements performed in specific locations (Mioduszewski et al., 2011). Two measurement points (at the road and the receptor sides) were determined within the study area (Fig. 1) to compare model-calculated road traffic noise values with the noise measurements. The main purpose was to check the consistency of the model calculations for two points before proceeding with model calculations for other locations in the study area. Based on the European Noise Directive, measurements were performed at each observation point for 24 h on September 22–29, 2022 in the open air at 4 m height from the ground level (END, 2002). Two Type-I sound level meters [Noise Level Measurement Device (SVAN 958, SV200) and Calibrator (SV 30A)] with the facility of integration, spectrum analysis, and data logging in real time were used. Before starting the measurements, all instruments were calibrated using an acoustic calibrator with a 94 dB(A) calibration value at 1 kHz.

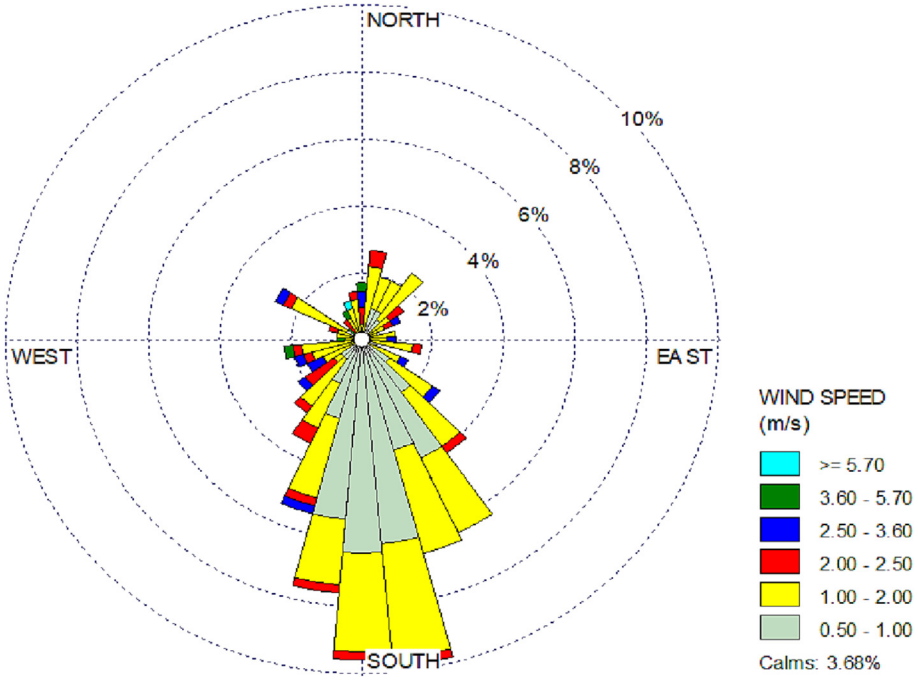

Fig. 5. Windrose plot for the measurement period.

2.2. Near-road air pollution dispersion modeling

In air pollution modeling, the emission rate per unit length of any road segment is usually calculated since it is the primary way that vehicle emissions are included in dispersion models. The emission factor represents the pollutant mass released per vehicle while moving on a unit length of a road. Since the US-EPAs testing procedures rely on calculating this amount, vehicle pollutant emissions are generally expressed as emission factors (Venkatram and Schulte, 2018). The European Environment Agency's Air Pollutant Pollution Inventory Guidebook (EMEP/EEA, 2020), the US-EPAs Emission Factors Catalogue (USEPA, 2007), and the Intergovernmental Panel on Climate Change Guidelines are the most widely used emission factor catalogs (IPCC, 2006). A tier in the EMEP/EEA guidance represents methodological complexity. Usually, Tier 1 is the simplest, Tier 2 is the intermediate level, and Tier 3 is the most data-intensive and complex method. In this study, due to the necessity of detailed data and statistics for analysis with other methods, emissions were calculated according to EMEP/EEA Tier 1 mean emission factors of NO_x (g/kg fuel) and typical fuel consumptions of vehicles (g/km). According to EMEP/EEA air pollutant emission inventory guidebook, there are three main vehicle categories; Passenger Cars (PC), Light Commercial Vehicles (LCV), and Heavy-Duty Vehicles (HDV) (EMEP/EEA, 2020). A report prepared by the Turkish Statistical Institute (TURKSTAT) was used to obtain the number of vehicles registered by fuel type at Turkiye in 2021 to classify the vehicles based on fuel types (TURKSTAT, 2021). According to this report, 26 %, 38 %, and 36 % of PCs were accepted as gasoline, diesel, and LPG fuel types, respectively. From the same report, 35 % and 65 % of LCVs were accepted as gasoline and diesel fuel types, respectively, while all HDVs were accepted as diesel fuel types. Since the D100 road section examined in this study is a main road, the powered two-wheeler fraction was negligible, and vehicle counts in this category were added to the PCs category. In this study, NO_x emission rates (g/m.s) were calculated using the above mentioned emission factors and vehicle statistics. Moreover, NO_2 emission rates were obtained through the multiplication of NO_x emission rates with the mass fractions of NO_2 in NO_x emissions for Euro 4 as stated in EMEP/EEA Guidebook (EMEP/EEA, 2020).

RLINE model code was developed for near-surface releases in a flat-terrain environment and contains formulations for vertical and lateral dispersion, low wind meander, and Monin-Obukhov similarity profile of surface winds, uses AERMET hourly surface meteorology (Snyder et al., 2013). US-EPA has integrated the RLINE model code and algorithms into the American Meteorological Society/Environmental Protection Agency Regulatory Model (AERMOD), a steady-state Gaussian air dispersion model based on planetary boundary layer theory. Uncertainties in Gaussian models and evaluations include observation error, model limitation, and input uncertainty. Model limitations are related to mathematical equations, computational applications, and built-in parameters that cannot adequately characterize complex physical processes and the variability involved. Gaussian modeling results are generally sensitive to wind data and atmospheric stability. For example, a slight change in the measured wind direction can cause significant concentration errors in the modeling (Zannetti, 2013). Models for ground-level area sources are also sensitive to land use/land cover characterization for albedo and surface roughness. Gaussian plume modeling is not expected to provide a precise fit between individual observations and predictions matched to time and space (Zannetti, 2013). The USEPA protocol for evaluating model performance concluded that "the precise time, location, and meteorological condition are negligible compared to the magnitude of the peak concentrations that occur" (USEPA, 1992). Specifically, air dispersion patterns can reasonably be expected to match statistical summaries (e.g., maximum, average, or percentiles) from concentrations measured in a given area over a selected period. In this study, the RLINE modeling program was used in two independent runs; one for the determination of the daily average NO_x, and the other for the determination of the bi-weekly average NO_2 grid-wise concentrations (in $\mu g/m^3$) for on-road vehicular emission loads. These model results were compared with the daily average real-time NO_x measurement results and bi-weekly average passive sampling NO_2 measurement results, respectively. After these analyses and the observation of compatibility between the average measurement and model results, the evaluated model results were used to represent the dispersion of traffic-related NO_x and NO_2 within the study area.

2.3. Road traffic noise modeling

Traffic noise is considered the most diffuse source of annoyance in urban areas. Different calculation methods have been developed to accurately model noise propagation, especially traffic-related noise propagation (Borelli et al., 2014). English standard CoRTN, German standard RLS 90, Italian standard C.N.R., CNOSSOS-EU, and French standard NMPB-Routes models can be listed as different road traffic noise calculation methods (Cannelli et al., 1983; CoRTN, 1988; Kephalopoulos et al., 2014; NMPB, 1996; RLS-90, 1990). According to the CNOSSOS-EU method, vehicles are grouped into four separate categories concerning their characteristics of noise emission: light motor vehicles ($\leq$ 3.5 tons), medium heavy vehicles (> 3.5 tons), heavy vehicles, and powered two-wheelers (Kephalopoulos et al., 2014). In this study, counted hourly vehicle numbers presented in Section 2.1.1 were adapted to the CNOSSOS-EU method's classification, and the CNOSSOS-EU method was used in modeling. Passenger Cars (PC), Light Commercial Vehicles (LCV), and Heavy-Duty Vehicles (HDV) were accepted as light motor vehicles ($\leq$ 3.5 tons), medium heavy vehicles (> 3.5 tons), and heavy vehicles, respectively. Vehicle count statistics are presented in Table 1.

In this study, the SoundPLAN 8.2 model was used to calculate the noise values associated with road traffic. The noise values were calculated for 10 m × 10 m grid size for the study area. A separate model run was performed for each day of the week with a 24-h continuous hourly vehicle numbers as an input. Average vehicle speeds were identified to the model as 110 km/h for light motor vehicles and medium-heavy vehicles and 90 km/h for heavy vehicles. The key inputs to the model are data on terrain and elevation, road traffic statistics, and road characteristics (slope, surface material). Traffic flow for the study area was chosen as continuous fluid flow, and the road surface was chosen as smooth asphalt in the model. The model software was utilized to compute the road slope using the digital ground model. The model calculated the noise exposure for each receptor point in the study area. The measurement data at the predetermined coordinates were compared to the model's calculated noise levels.

3. Results and discussion

3.1. Simultaneous noise, air pollution, and vehicle number relationship

Real-time measurements were performed for one week with the measurement infrastructure located at the road and receptor sides of the barrier. The one-week average noise values, together with NO, NO_2, NO_x, and O_3 concentrations obtained during this period, are given in Table 2.

Simultaneous hourly measurement results for noise, NO_x, O_3, and vehicle numbers are presented in Fig. 6. The difference between the simultaneous noise measurements on the road and the receptor sides of the

Table 1
Hourly vehicle counts on the D100 road section.

Day	Vehicle/day	Hourly vehicle numbers [day (07:00–19:00)/evening (19:00–23:00)/night (23:00–07:00)]		
		Light motor vehicles	Medium heavy vehicles	Heavy vehicles
23.09.2022 Friday	23,718	994/908/238	270/242/68	88/59/26
24.09.2022 Saturday	23,786	984/1016/294	258/256/82	46/7/26
25.09.2022 Sunday	21,478	842/1056/280	220/266/78	30/7/24
26.09.2022 Monday	22,818	948/710/228	270/204/64	130/96/33
27.09.2022 Tuesday	22,962	960/670/242	274/192/70	130/94/34
28.09.2022 Wednesday	23,830	1018/622/254	290/178/74	140/88/35

Table 2
One-week averages of measured parameters during the real-time measurement period.

Position to the barrier	NO ($\mu g/m^3$)	NO_2 ($\mu g/m^3$)	NO_x ($\mu g/m^3$)	O_3 ($\mu g/m^3$)	L_{Aeq} (dBA)
Road side	44.17	23.75	67.92	17.20	73.01
Receptor side	28.16	23.92	52.10	27.27	59.98

barrier generally remains constant. Hourly noise measurement results indicated that the noise barrier resulted in a 13.1 dB(A) average noise level reduction during the measurement period at the measurement point, approximately 10 m receptor side of the barrier and 4 m high. The average vehicle number per hour was 1300 between 08:00–19:00, dropping to 185 between 02:00–06:00. In these periods, approximately 10 dB(A) reduction in noise level was observed. The correlation coefficients (r) between hourly vehicle numbers and hourly noise levels were found to be 0.94 and 0.86 for the road and receptor sides, respectively. Since the predominant noise source was the road traffic in the study area, the high correlations observed between the noise levels and the vehicle numbers are expected. However, possibly due to reasons such as additional contributions from some other sources and/or participation of these air pollutants in chemical reactions that are very sensitive to micrometeorological variables, such a stable relationship with a high correlation was not observed between hourly vehicle numbers and hourly NO_x or O_3 concentrations.

The real-time measurement results indicated that the noise barrier has an average 23 % reduction effect on NO_x concentration at 5 m behind the barrier. Hooghwerff et al. (2010) measured 20 % reduction for NO_x at 10 m behind the reference barrier (Hooghwerff et al., 2010). Baldauf et al. (2008) found 15–50 % reduction in CO and PM number concentrations downwind of the barrier as the wind blows from the lane (Baldauf et al., 2008). The NO_x concentrations were observed at the highest levels between 03:00 and 12:00. While NO_x concentrations reached the lowest level between 12:00 and 18:00, O_3 concentrations were observed at the highest levels during the same period. Between 18:00 and 00:00, the NO_x concentrations increased again. Besides, hourly vehicle numbers increase rapidly after 06:00, remain in high numbers between 08:00 and 19:00, and decrease rapidly after 19:00. Although hourly vehicle numbers between 12:00 and 18:00 are at similar levels, a sudden decrease in NO_x and a sudden increase in O_3 concentrations were observed. Elevated ozone concentrations in polluted regions, including road traffic-related ozone formation, occur through the following sequence of reactions. The system is initiated by the various VOCs or CO with the OH radical (Eq. (1) and Eq. (2)). NO is converted into NO_2 by RO_2 (peroxy) or HO_2 (hydroperoxyl) radicals, and these reactions regenerate OH (Eq. (3) and Eq. (4)). Then, NO_2 is photolyzed with sunlight and generate atomic oxygen. Atomic oxygen reacts with O_2 to create O_3 (Eq. (5) and Eq. (6)). However, nearby to considerable emission sources of NO at nighttime, ozone concentrations are depressed through a reaction with NO (Eq. (7)). During the daytime, this reaction is usually balanced by the photolysis of NO_2 (Eq. (5) and Eq. (6) (Sillman, 2003).

$$VOC + OH + O_2 \rightarrow RO_2 + H_2O \quad (1)$$

$$CO + OH + O_2 \rightarrow HO_2 + CO_2 \quad (2)$$

$$RO_2 + NO + O_2 \rightarrow VOC_{secondary} + HO_2 + NO_2 \quad (3)$$

$$HO_2 + NO \rightarrow OH + NO_2 \quad (4)$$

$$NO_2 + h\nu \rightarrow NO + O \quad (5)$$

$$O + O_2 + M \rightarrow O_3 + M \quad (6)$$

$$NO + O_3 \rightarrow NO_2 + O_2 \quad (7)$$

The sudden decrease in NO_x concentrations and the sudden increase in O_3 concentrations between 12:00 and 18:00 are caused by the effect of sunlight through photocatalytic reactions (Eq. (5) and Eq. (6)). High O_3 concentrations decrease in the evening and go down to zero at night as expected (Eq. (7)) (Sillman, 2003). Studies in China indicated that local

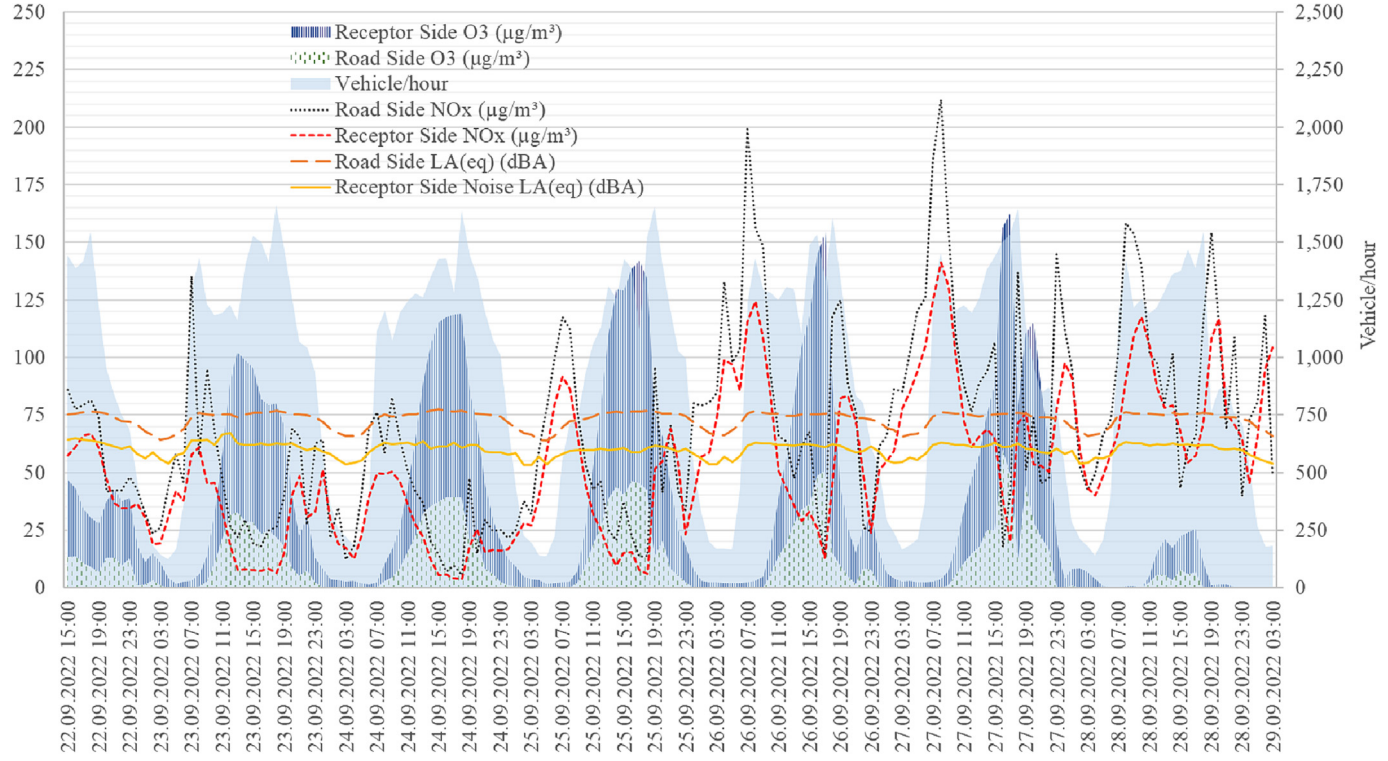

Fig. 6. Real-time hourly measurement results for noise, NO_x, O_3, and vehicle numbers.

O_3 formation is sensitive to VOCs in the morning and NO_x in the afternoon. In general, cities are VOC sensitive; outer suburbs are NO_x sensitive, and inner suburbs are VOC and NO_x sensitive (Xu et al., 2022).

The relationship among NO, NO_2, and O_3 concentrations during the measurement period is shown in Fig. 7. The one-week average ratios of roadside and receptor side concentrations for NO_x, NO, and NO_2 are 1.30, 1.57, and 0.99, respectively. Besides, O_3 concentrations were lower at the roadside of the barrier than those on the receptor side. The one-week average ratio of the receptor side concentrations to the roadside concentrations for O_3 is 1.59. Since the NO_2 concentrations are similar on both sides of the barrier, the O_3 catalytic production rate is expected to be similar (Eqs. (5)-(6)). However, considering Eq. (7), higher NO concentrations on the roadside are thought to be the reason for more O_3 destruction and lower concentrations at the roadside. In the vicinity of significant NO emissions, the result is a net conversion of O_3 to NO_2. Ozone is depressed immediately downwind of the road traffic and becomes elevated as the plume moves further downwind. Since there is no photocatalytic production at night, the reaction in Eq. (7) also leads to ozone removal (Sillman, 2003).

Ambient O_3 concentrations get affected by atmospheric stability levels. Since the more unstable the atmosphere is, the greater the dilution of the pollutant, the mechanical turbulence in the atmosphere dramatically affects the concentration of a pollutant. A stable atmosphere resists turbulence, but an unstable atmosphere enhances mechanical turbulence (NOAA, 2022). Ozone concentrations are significantly influenced by changes in the weather. Warm, sunny days with stagnant air allow ozone to build more quickly. On the other hand, when it is cloudy, cool, wet, or windy, ozone formation is more limited (USEPA, 2021). Fig. 4 shows that cloudiness was high almost all the time during the last day of the real-time measurement period (September 28, 2022). An apparent reduction in O_3 concentrations is evident due to decreased UV-dependent ozone reactions. During the daytime (07:00–19:00), at low wind conditions (< 2 m/s), unstable conditions are dominant, and the NO_x concentrations tend to be diluted and reduced. At nighttime (19:00–07:00), stable conditions dominate, and the atmosphere resists turbulence, so the NO_x concentrations increase. While the hourly vehicle number and the NO_x concentration trends between 19:00 and 07:00 were generally consistent on September 22–23, this was not the case on September 24–25 (Fig. 6). This difference may be due to the lower nighttime temperatures and more stable atmospheric conditions in the latter period (Fig. 4).

3.2. Passive tube measurement results

Passive tube measurement results for NO_2, O_3, Benzene, Toluene, Ethyl Benzene, mp-Xylene, and o-Xylene are given in Figs. 8–11 (Fig. 8, Fig. 9, Fig. 10, and Fig. 11). The BTEX sample tube at point 2 could not be analyzed due to the deformation of the absorbent material in the field conditions. The results in these figures indicate that the bi-weekly average values fluctuate among the passive tubes at the same distance from the barrier. The complex turbulence in front of the barrier and the recirculation zone behind the barrier can cause these fluctuations. The recirculation zone extends about 6 barrier heights behind the barrier (Venkatram and Schulte, 2018), and considering that the existing barrier in the study area is 4 m high, the recirculation zone covers approximately 24 m distance from the barrier.

The passive sampler tubes at sampling point 4 and 8, located on the roadside and the receptor sides of the barrier, were almost at the same positions and heights as the real-time measurement devices. For this reason, passive tube-based bi-weekly average NO_2 concentrations can be compared with the real-time-based one-week average NO_2 concentrations. The passive sampling and the average real-time NO_2 concentrations at the roadside of the barrier were 25.2 $\mu g/m^3$ ($\pm$ 2) and 23.75 $\mu g/m^3$, respectively, while they were 27.9 $\mu g/m^3$ ($\pm$ 2.2) and 23.92 $\mu g/m^3$ at the receptor side of the barrier, respectively. These results show that the measurement results obtained by passive samplings can be used for the dispersion modeling of NO_2 pollutant. Some differences between the one-week real-time and bi-weekly passive sampling measurements for NO_2 and O_3 can originate from meteorological conditions such as wind direction, cloudiness, and temperature between the first and the second weeks (Fig. 4). The average ambient temperatures were 15 °C and 17.4 °C during the first and the second weeks of the measurement period, respectively, and temperature directly influences concentrations of these pollutants by speeding up the rates of chemical reactions (Coates et al., 2016).

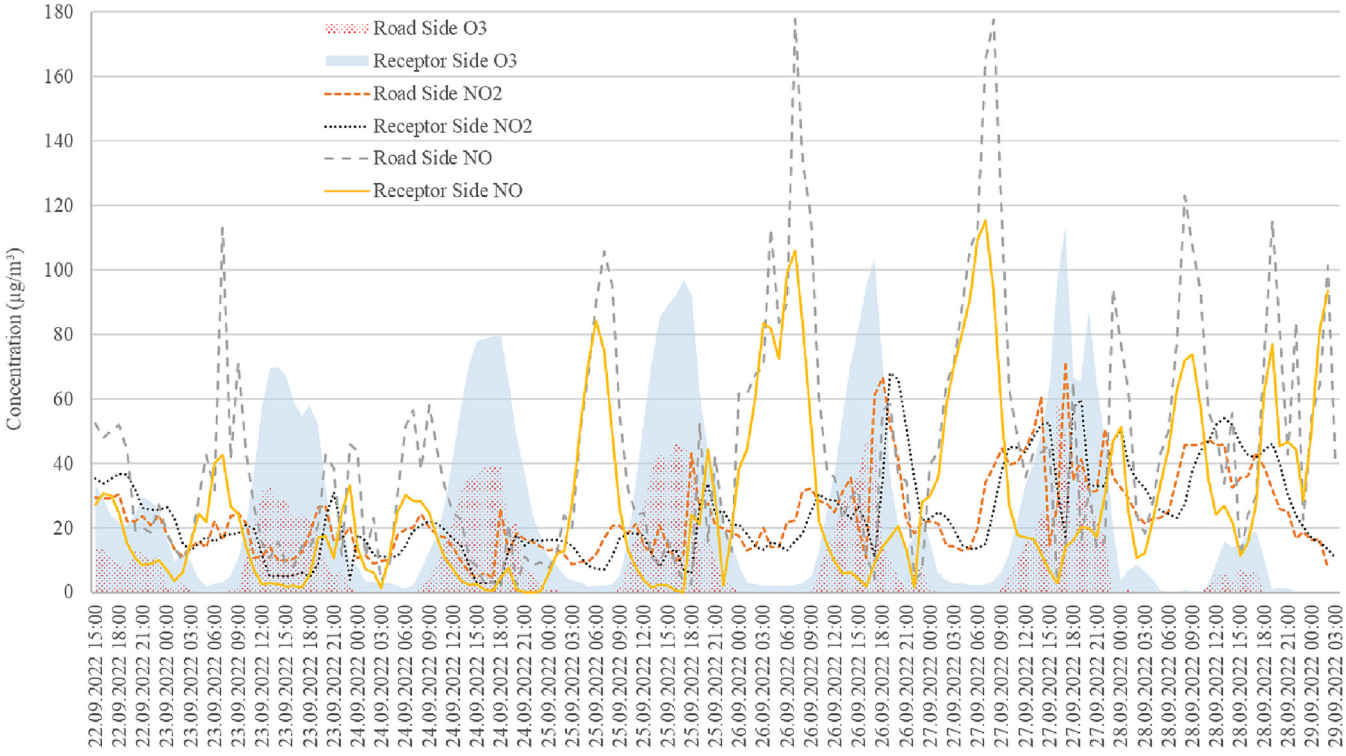

Fig. 7. Real-time NO, NO_2, and O_3 Measurement Results (September 22–29, 2022).

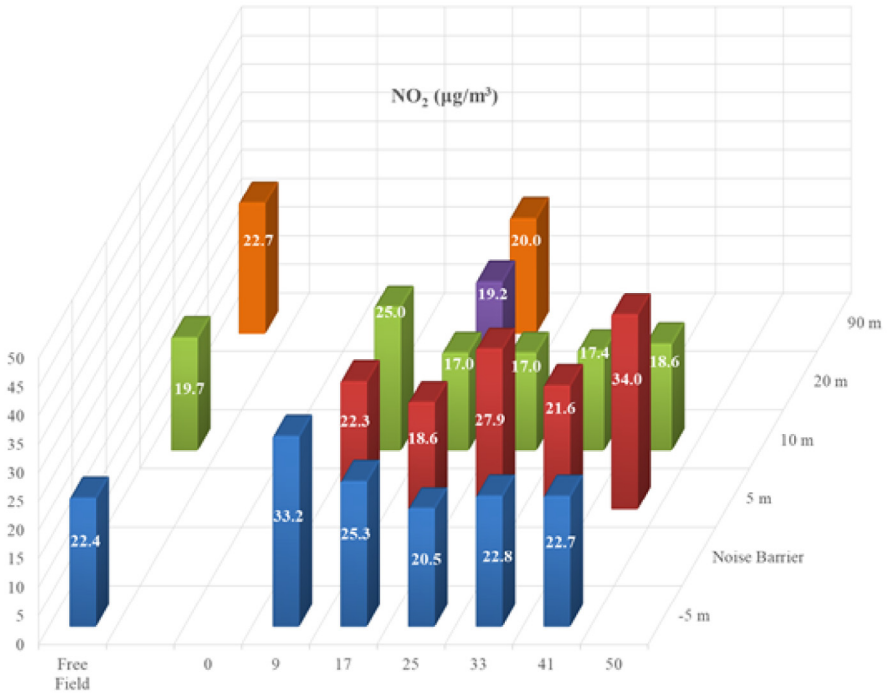

(a)

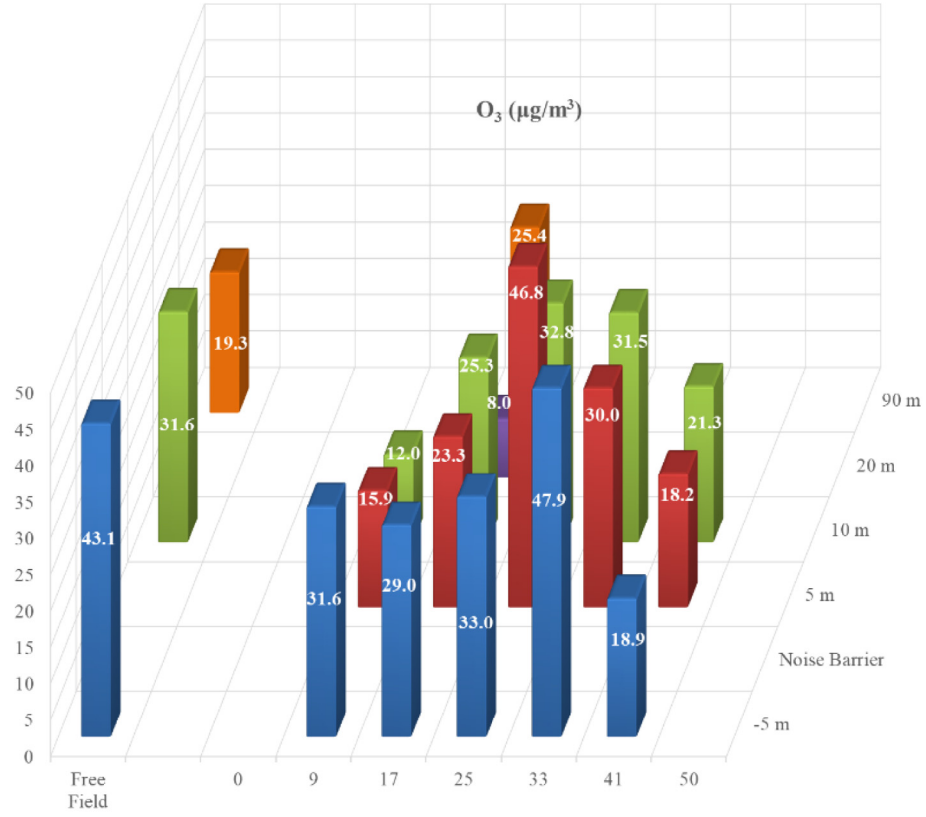

(b)

Fig. 8. The NO_2 and O_3 passive tube measurement results (X;Y = 0;0 represents the beginning point of the noise barrier from the west side).

Taking averages of concentrations measured by the passive samplers within the same distance from the barrier might be more informative. Fig. 12.a presents the passively measured average concentrations for NO_2 and O_3 in front of and behind the barrier at the same distance from the barrier, while Fig. 12.b presents the passively measured free field concentrations for the same pollutants. The results indicate

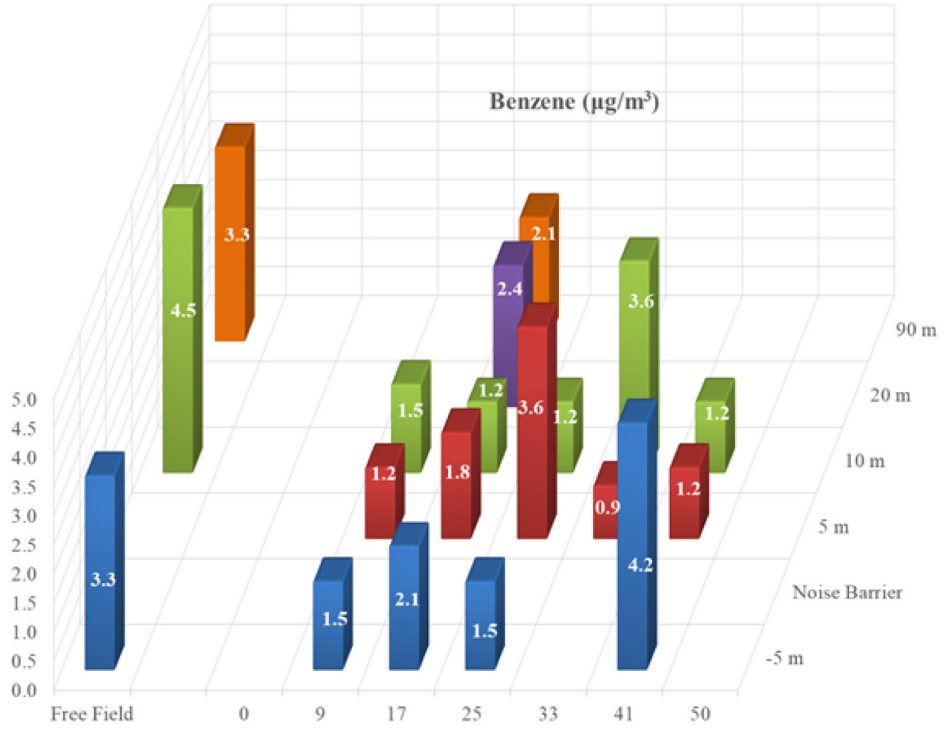

(a)

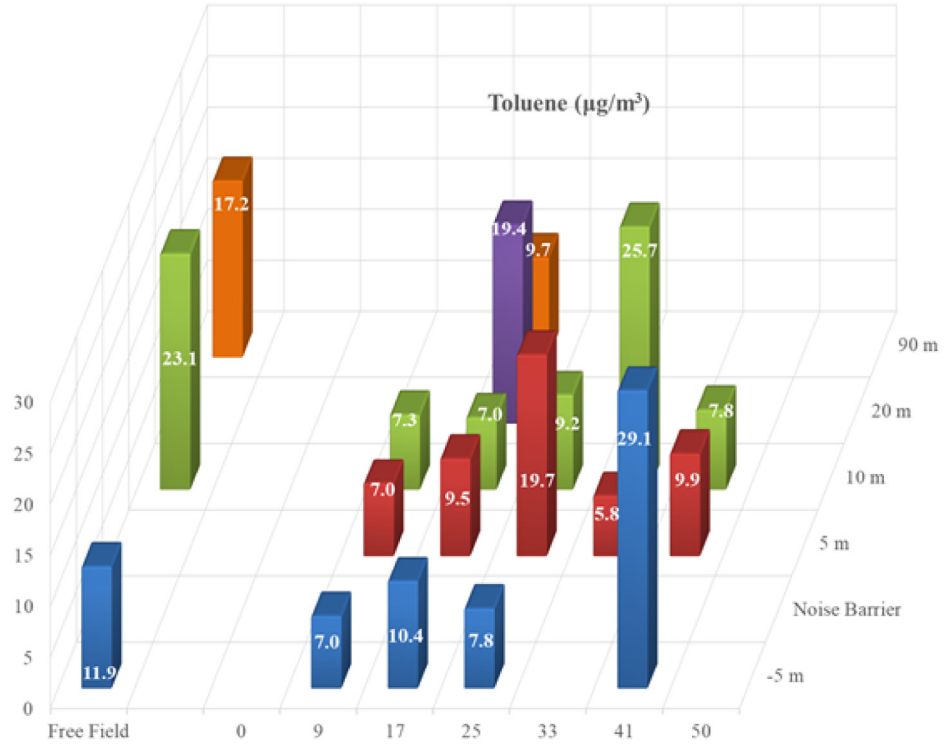

(b)

Fig. 9. Benzene and Toluene passive tube measurement results (X;Y = 0;0 represents the beginning point of the noise barrier from the west side).

reductions of 0 % to 24 % for NO_2 and 16 % to 23 % for O_3 for the barrier case (Fig. 12.a) and reductions of 0 % to 12 % for NO_2 and 27 % to 55 % for O_3 for the free field case (Fig. 12.b). Therefore, it can be concluded that the barrier effect is only evident for NO_2 pollution. BTEX results indicate 5 % to 29 % reductions for the barrier case (Fig. 13.a) and increasing concentrations for the free field case (Fig. 13.b). Therefore,

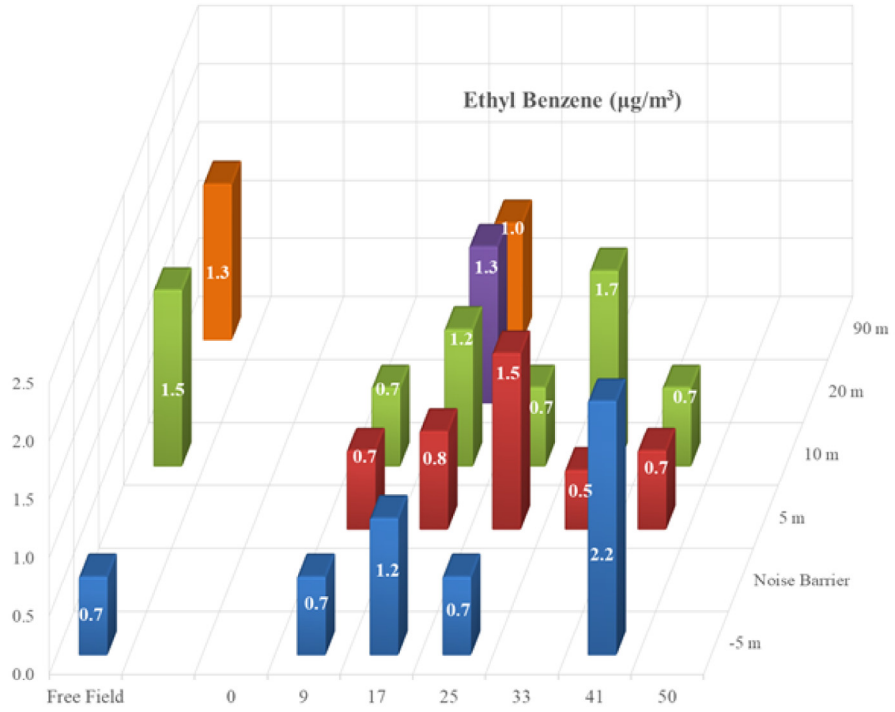

(a)

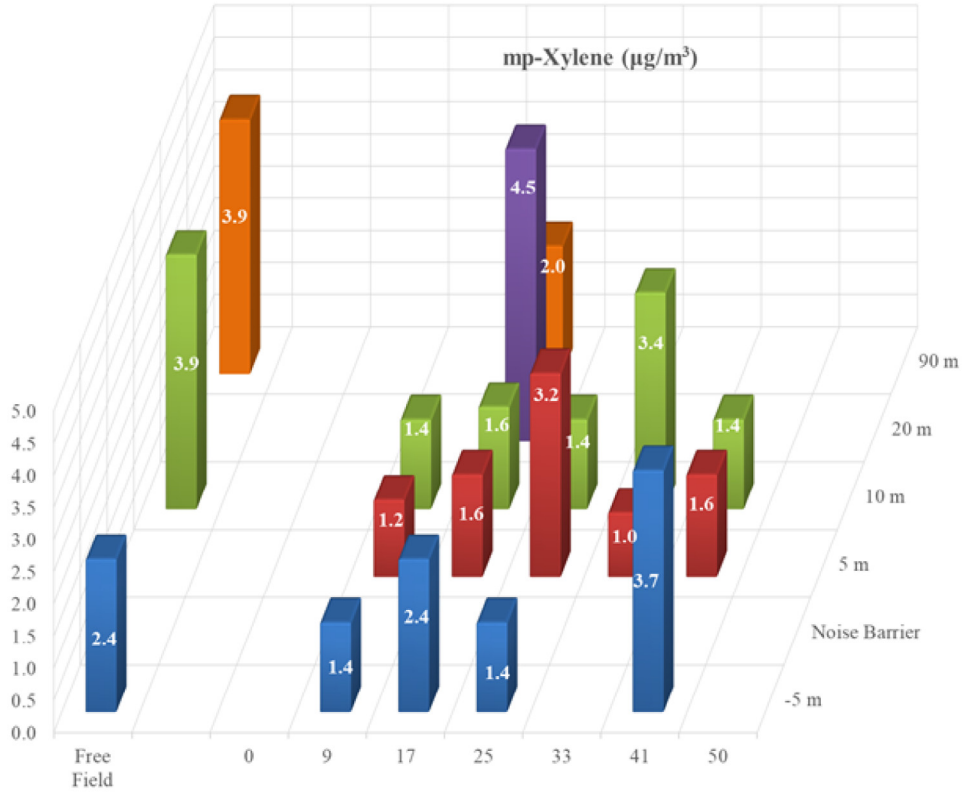

(b)

Fig. 10. Ethyl Benzene and mp-Xylene passive tube measurement results (X;Y = 0;0 represents the beginning point of the noise barrier from the west side).

the reductions in all of the BTEX concentrations resulting from the existence of the barrier in comparison to the free field concentrations are evident. The passive sampling measurement results obtained for the sampler located 20 m behind the barrier were excluded from these figures and the statistical calculations since there is only one sample at that distance, and an average value representing the effect of the barrier

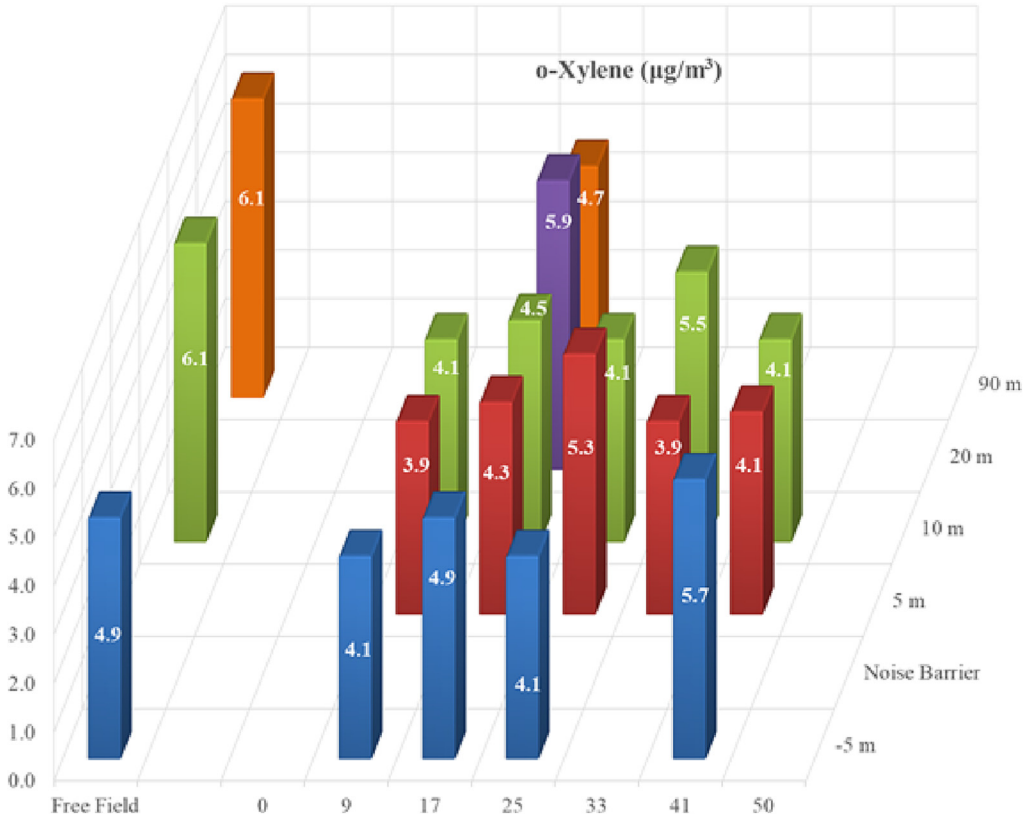

Fig. 11. o-Xylene passive tube measurement results (X;Y = 0;0 represents the beginning point of the noise barrier from the west side).

cannot be obtained. In addition, there is no free field measurement value for that distance to compare with the barrier case. Ranasinghe et al. (2019) found that combining vegetation and a solid sound wall (combination barrier) caused 29 % and 2 % relative reductions of averaged NO and NO_2 concentrations, respectively (Ranasinghe et al., 2019).

3.3. Near-road air pollution dispersion modeling and evaluation

Daily average real-time NO_x concentration measurement results were compared with RLINE model calculation results. Correlation coefficients (r) were calculated as 0.96 and 0.93 for the roadside and the receptor side concentrations, respectively. Moreover, geometric mean (m_g), a factor

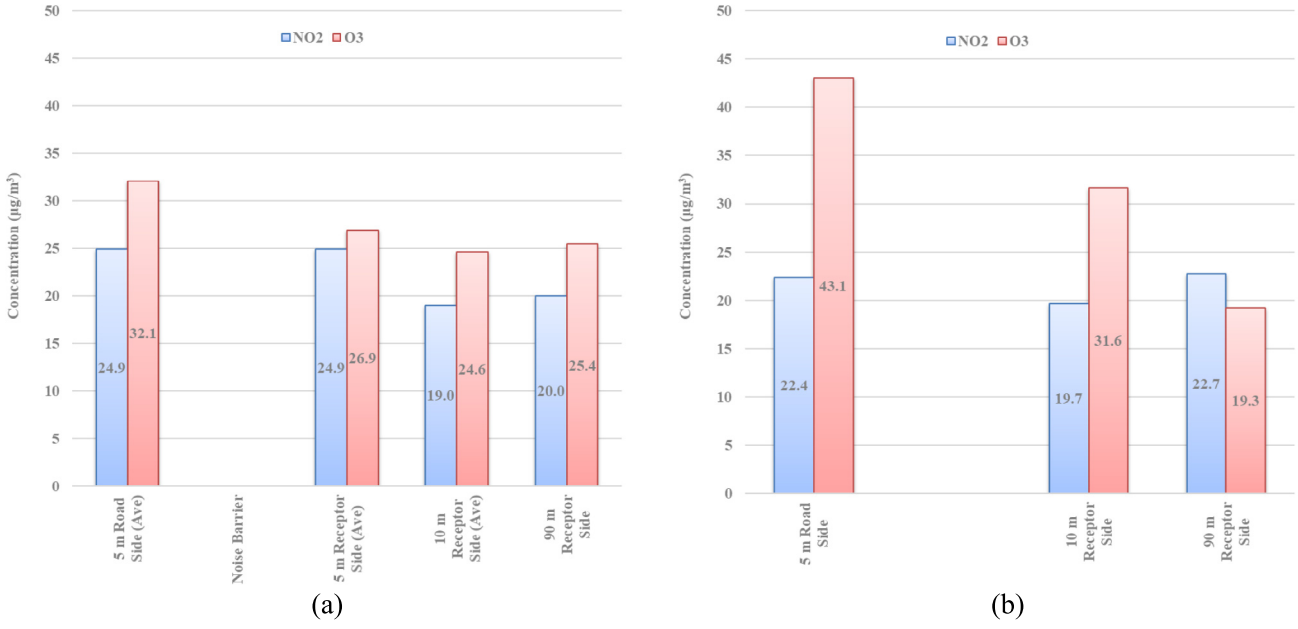

Fig. 12. NO_2 and O_3 concentrations with the noise barrier (a) and in the free field (b).

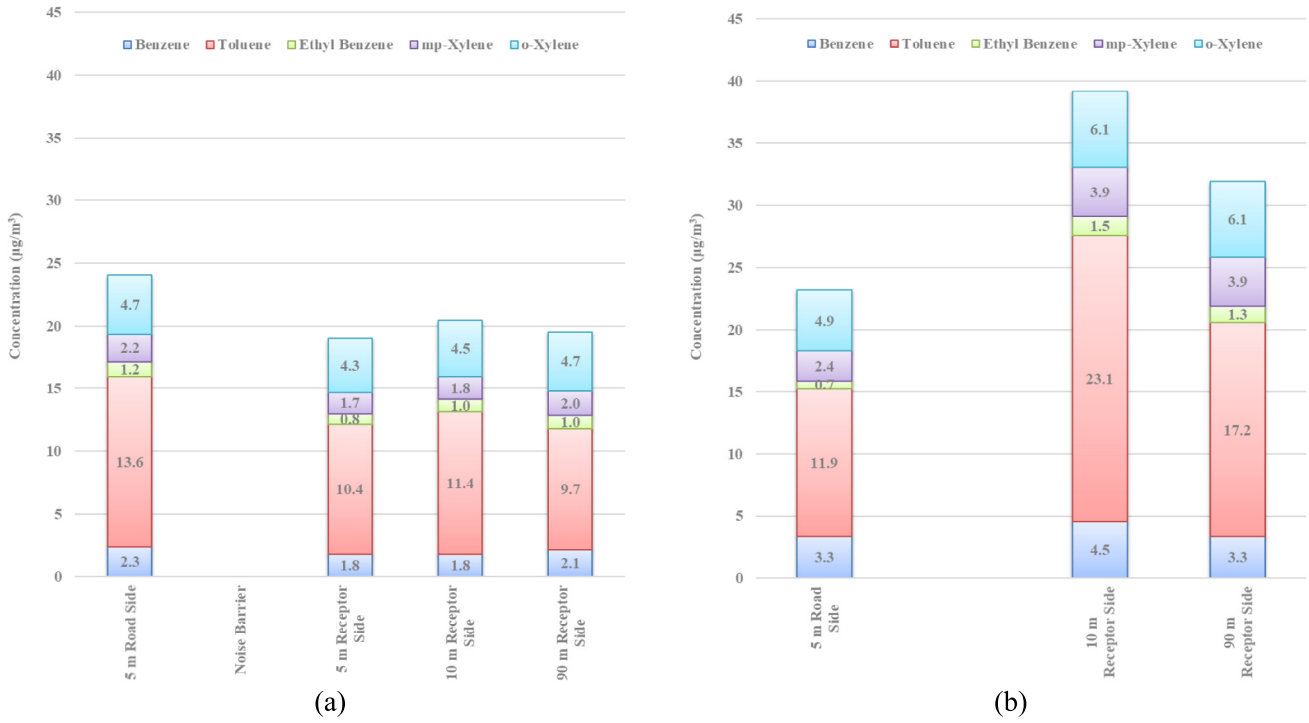

Fig. 13. BTEX concentrations with the noise barrier (a) and in the free field (b).

of two (FAC2), and determination coefficient (r^2) values were determined as 1.16, 100 %, and 0.92, respectively, for the roadside values. The same parameters for the receptor side values were determined as 1.03, 100 %, and 0.86, respectively. As can be seen in Fig. 14, there is a strong correlation between the measured and the calculated NO_x concentration results.

Patterson and Harley (2019) evaluated the RLINE dispersion model against yearlong hourly NO_x and black carbon (BC) measurements at two near-road monitoring sites in the San Francisco Bay Area. The overall agreement between model predictions and observations for 24-h average NO_x and BC was reasonably good, with >90 % of predictions within a factor of two (FAC2) of the near-road monitoring data (Patterson and Harley, 2019). Amini et al. (2016) evaluated the performance of two different barrier models developed for stable and unstable atmospheric conditions with measurements. The geometric mean (m_g), a factor of two (FAC2), and determination coefficient (r^2) values for the stable conditions were found to be 0.95, 96 %, and 0.52, respectively. The same parameters for the unstable conditions were found to be 0.95, 98 %, and 0.53, respectively (Amini et al., 2016).

Bi-weekly average NO_2 passive sampler measurement results were compared with bi-weekly average NO_2 model calculated results, as shown in Fig. 15. The results in this figure are presented for every passive sampling point. (X;Y) = (0;0) represents the beginning point of the noise barrier from the west side, while (X;Y) values under every bar represent the points of passive sampling tubes relative to the point (0;0). As can be seen, the model and measurement results are generally compatible except for a few points, especially close to the ends of the barrier. These might be related to the connection roads (not defined in the model) at the west and east side of the barrier that are used as entrances and exits to some nearby

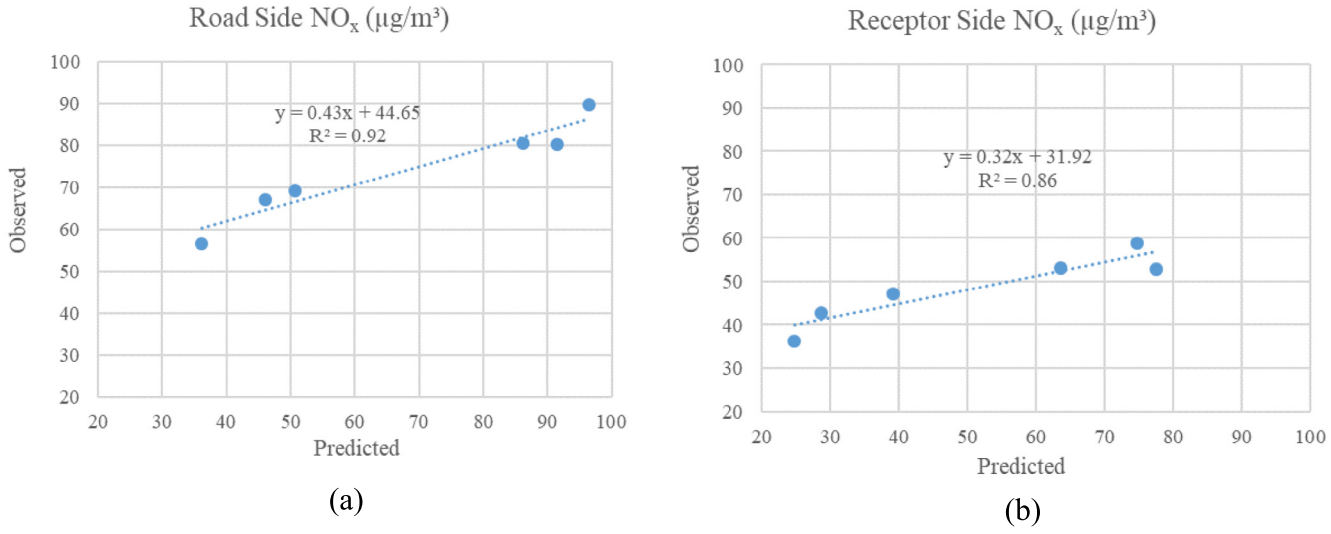

Fig. 14. RLINE model comparison with daily average NO_x measurement results.

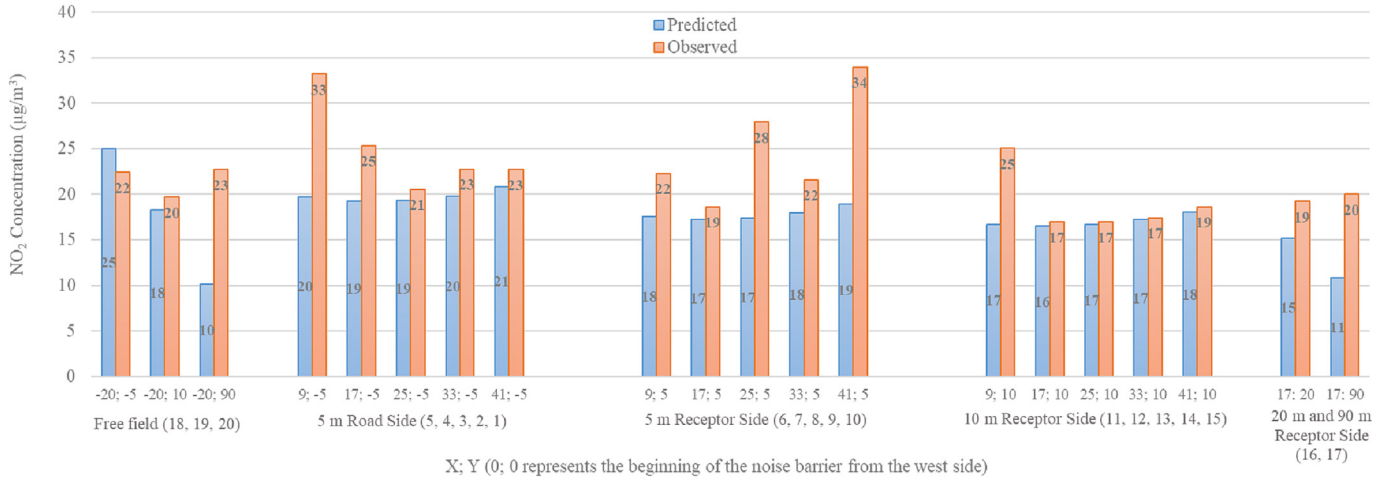

Fig. 15. RLINE model calculated and passively measured average NO_2.
(Numbers in the parenthesis represent the measurement locations in Fig. 1).

facilities. Higher fluctuations between the observed and predicted results at 5 m behind the barrier might be related to the recirculation zone formation just behind the barrier. While the measurement and model results for the free field at points close to the D-100 road were compatible, the measurements at 90 m behind the road were much higher than the model result. A similar discrepancy is also evident at 90 m behind the barrier. These mismatches can originate from some unidentified source contributions or micro-meteorological conditions that were not considered in the model.

3.4. Road-traffic noise modeling and evaluation

SoundPLAN 8.2 modeling software was used to calculate the noise levels at measurement points by considering the road traffic as the only noise source. Noise levels were calculated in the 10mx10m grid sizes. Road traffic statistics, road properties (slope, surface material), terrain and elevation data, number and locations of buildings are the primary inputs to the model. The measurement and modeling results at measurement points were compared. The roadside and the receptor side noise measurement and modeling results are presented in Fig. 16 and Fig. 17, respectively. The results indicated that the observed and the predicted noise values are compatible, and the average differences for the roadside and the receptor side are 1.53 dB(A) and 1.09 dB(A), respectively. The results showed that most of the $L_{A(eq)}$ values calculated using the SoundPLAN 8.2 model are within the acceptable accuracy range of ±2 dB(A) (Nast et al., 2014) for both sides of the barrier. Besides, according to a US Department of Transportation report, road noise modeling results are acceptable if the uncertainty level is <3 dB(A) (Tsai et al., 2019; USDT, 2010). Correlation coefficients (r) were calculated as 0.97 and 0.89 for the roadside and the receptor side noise values, respectively.

3.5. Simultaneous effects of the noise barrier on traffic-sourced NO_x and noise

The model results of near-road NO_x and noise dispersion were confirmed by the weekly real-time measurement results. The weekly average near-road NO_x and noise dispersion model results are presented in Fig. 18 and Fig. 19, respectively. A reduction in NO_x concentrations at the receptor side of the barrier is evident due to its leeward location (Fig. 18). As can be seen, in the free field conditions with no barrier, the average NO_x concentration values observed at a distance approximately 100 m from the road midline were observed at a distance approximately 70 m from the road midline in the section where the barrier is located. Compared to the free field concentrations, the values behind the barrier are approximately 10–20 %, 12–30 %, and 13–33 % lower at distances 0–20 m, 20–50 m, and 50–70 m, respectively. Ning et al. (2010) found that particle mass, CO, NO_2, and Black Carbon (BC) concentrations reached background levels at distances 250–400 m further compared to 150–200 m at sites without roadside noise barriers. They observed that the particle number concentrations were 45–50 % of those measured at similar downwind distances of freeways without roadside barrier (Ning et al., 2010).

Daily average noise was represented as L_{den}, which is a descriptor of noise level based on energy equivalent noise level (L_{eq}) over a whole day with a penalty of 10 dB(A) for nighttime (23:00–07:00) noise and an

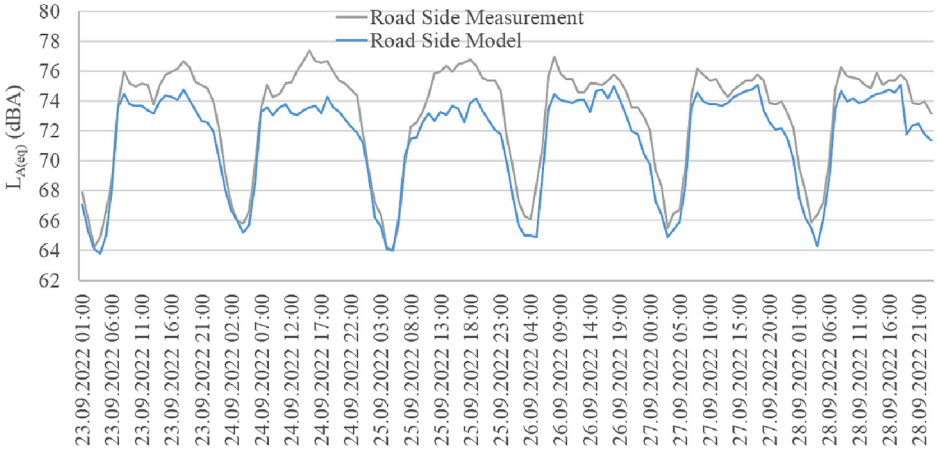

Fig. 16. Roadside noise measurement and model results.

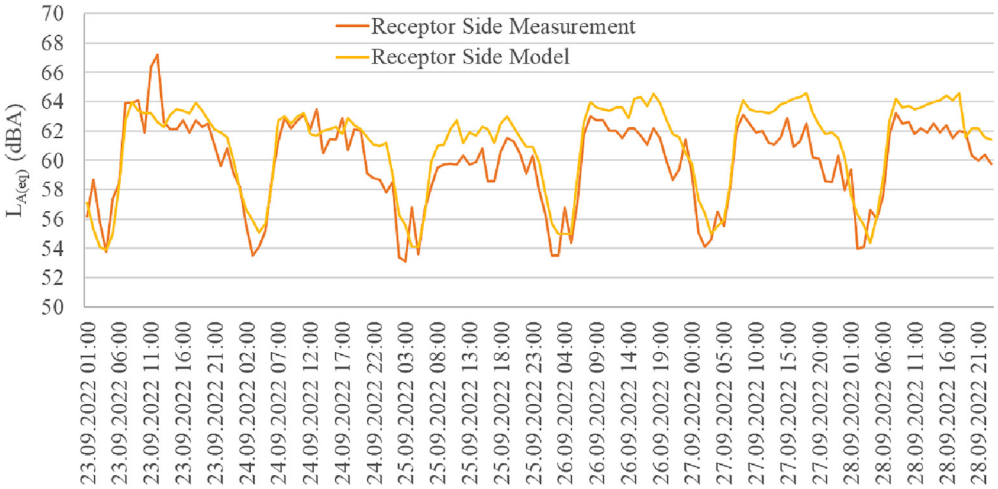

Fig. 17. Receptor side noise measurement and model results.

additional penalty of 5 dB(A) for evening time (19:00–23:00) noise. Considerable noise reduction levels at the receptor side of the barrier are evident (Fig. 19). Compared to the free field noise values, the values behind the barrier are approximately 17–35 %, 12–19 %, and 2–15 % lower at distances 0–10 m, 10–20 m, and 20–70 m, respectively.

Calculated weekly average noise and NO_x values under the free field conditions were compared in Fig. 20.a. They are highly correlated with a correlation coefficient (r) of 0.78. Davies et al. (2009) measured bi-weekly average roadside NO_2 and NO_x concentrations and short-term average noise levels ($L_{eq,5min}$) at 103 locations on roads with variable traffic. They found Pearson correlation coefficients between $L_{eq,5min,}$ and NO_2 and between $L_{eq,5min,}$ and NO_x as 0.53 and 0.64, respectively. Ising et al. (2004) calculated the correlation coefficient of noise and NO_2 measurements as 0.84. Using the modeled values for both noise and NO_2, Klaeboe et al. (2000) found the correlation coefficient as 0.46 between them. The result of a similar calculation obtained in this study for the receptor points approximately 30 m East of the western end of the barrier (the barrier midpoint is 25 m East) is given in Fig. 20.b. The correlation coefficient

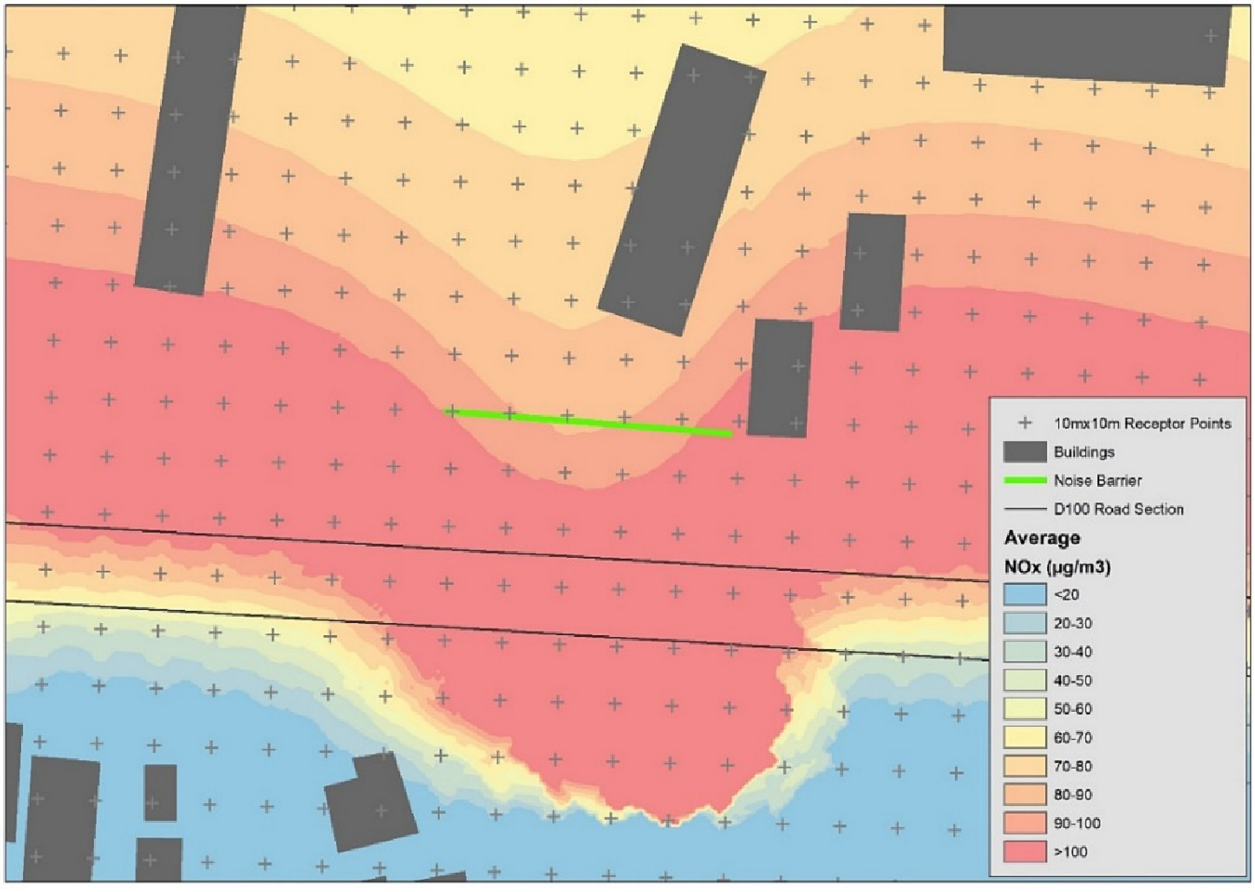

Fig. 18. The weekly average near-road NO_x dispersion model results.

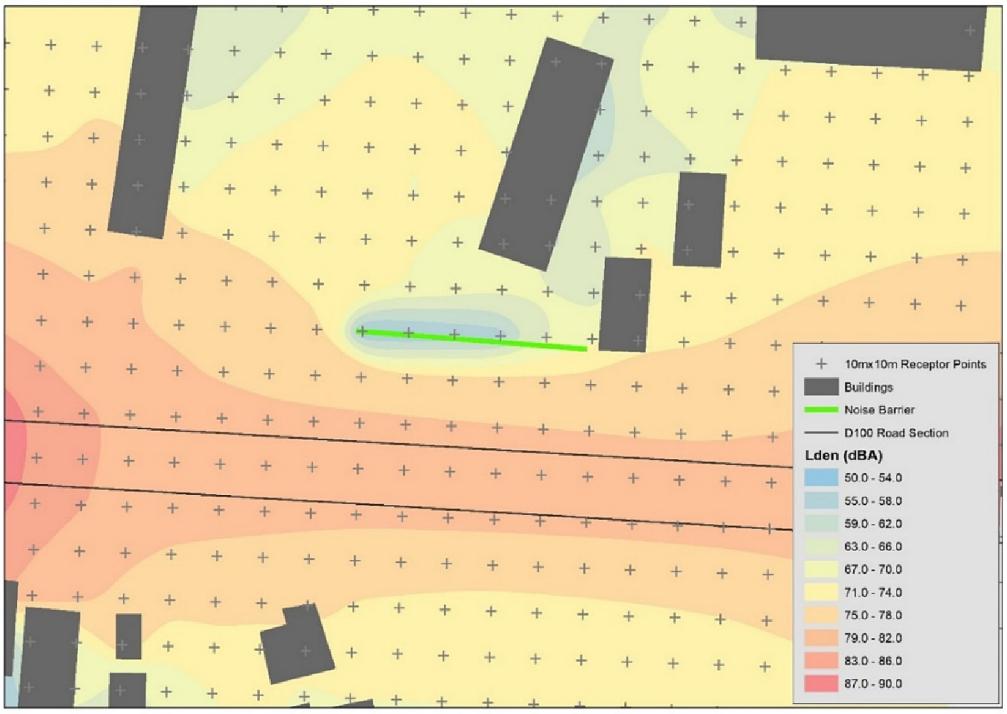

Fig. 19. The weekly average noise dispersion model results.

between the model-calculated noise and NO_x values decreased to 0.34 when the barrier existed. Although the noise barrier has a reduction effect on both noise and NO_x, the observed low correlation points out that their dispersion mechanisms are different. The air pollution dispersion behind the barrier can be represented better due to the higher-resolution mathematical analysis used in the model.

4. Conclusion

Noise barrier use, considered within the scope of measures to reduce the spread of environmental noise, is one of the common solutions to control road noise. Many studies have shown that noise barriers cause a reduction in air pollutant concentrations behind a barrier at close distances to the road. In this study, the simultaneous effects of a specific noise barrier application on near-road noise and air pollution at a specific location were investigated. In this context, air pollution, noise, and meteorological parameters were measured simultaneously near a 50 m long, 4 m high glass fiber reinforced concrete noise barrier on a highway section. At the same time, the road traffic was recorded on video for the determination of motor vehicle statistics. Real-time NO, NO_2, NO_x, O_3, and noise measurements were carried out simultaneously at two points located on both sides of the barrier for a week. In addition, passive tube samplers were used to determine the cumulative average concentrations of NO_2, O_3, and BTEX pollutants at 20 points for two-weeks period. After the field studies, vehicle statistics and meteorological data were processed to be used as inputs in RLINE and SoundPLAN 8.2 modeling software for NO_x and noise dispersion calculations. The measurement results were found to be compatible with the model results. Therefore, the simultaneous effects of the noise barrier on noise and air pollution dispersion were evaluated with these models.

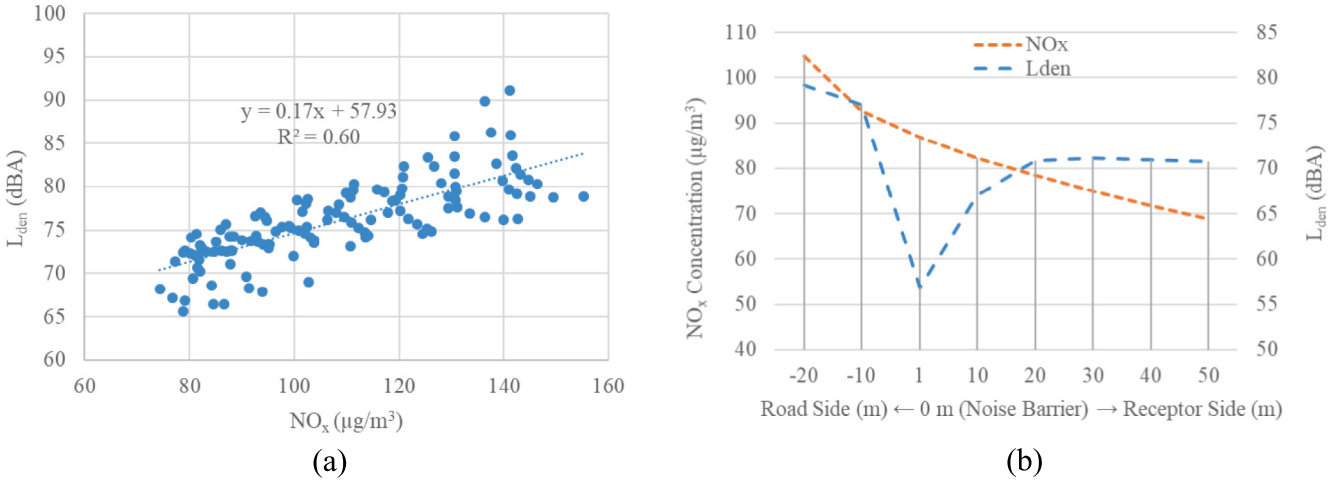

Fig. 20. Comparison of model calculated noise and NO_x values (a) under the free field conditions, (b) with the noise barrier.

Generally, low wind speeds were dominant and calm conditions were observed during the two weeks measurement period. Simultaneous noise measurements, performed for model and measurement consistency check at two points, indicated 13.1 dB(A) average noise level reduction between 5 m road and 10 m receptor sides of the barrier at 4 m height. The average differences between the noise measurement and modeling results were determined as 1.53 dBA and 1.09 dBA for the roadside and the receptor side of the barrier, respectively. The correlation coefficients between the hourly vehicle numbers and the hourly noise measurement values for the road and the receptor sides of the barrier were found to be 0.94 and 0.86, respectively. The correlation coefficients (r) between the noise measurement and model calculated results were found as 0.97 and 0.89 for the roadside and the receptor side, respectively.

Real-time weekly average measurement results indicate that the noise barrier examined in this study has an average 23 % reduction effect on NO_x concentration at 5 m from the barrier at the receptor side. However, possibly due to reasons such as additional contributions from some other sources and/or participation of these air pollutants in chemical reactions that are very sensitive to micrometeorological variables, such a stable relationship with a high correlation was not observed between the hourly NO_x or O_3 concentrations and hourly vehicle numbers. Because of sunlight-related photocatalytic reactions, sudden fluctuations were observed in NO_x and O_3 concentrations even with approximately constant vehicle numbers between 12:00 and 18:00. The passive sampling results indicate reductions of 0 % to 24 % for NO_2 and 16 % to 23 % for O_3 for the barrier case and reductions of 0 % to 12 % for NO_2 and 27 % to 55 % for O_3 for the free field case. Therefore, it can be concluded that the barrier effect is only evident for NO_2 pollution. The passive sampling results also indicate 5 % to 29 % reductions for BTEX pollutants with the barrier case, while no reductions were indicated for the free field case. Therefore, the effectiveness of the barrier for BTEX pollutants is clearly evident.

Daily average real-time NO_x measurement results were compared with RLINE model calculation results at the measurement points, and the correlation coefficients (r) 0.96 and 0.93 were obtained for the roadside and the receptor side concentrations, respectively. The passive sampler NO_2 measurement results performed at two points at both sides of the barrier are compatible with the averages of the real-time NO_2 measurement results performed at locations very close to these points. Therefore, the passive sampler NO_2 measurement results were used for comparisons with model-calculated results. In this context, bi-weekly average passive sampler NO_2 measurement results were compared with bi-weekly average NO_2 model calculated results. The model and measurement results are generally compatible except for a few points especially close to the ends of the barrier and also at 90 m behind the barrier. The possible reasons for the discrepancies are discussed in Section 3.3.

Comparisons between the free field noise values and the values behind the barrier indicated approximately 17–35 %, 12–19 %, and 2–15 % reductions at distances 0–10 m, 10–20 m, 20–70 m, respectively. Similarly, comparisons between the free field NO_x values and the values behind the barrier indicated approximately 10–20 %, 12–30 %, and 13–33 % reductions at distances 0–20 m, 20–50 m, and 50–70 m, respectively. Under the free field conditions in the study area, the model-calculated weekly average noise and NO_x values were compared and found to be highly correlated with a correlation coefficient (r) of 0.78. However, the correlation coefficient between the model-calculated weekly average noise and NO_x values decreased to 0.34, where the barrier exists. Although the noise barrier showed a clear reduction effect on both noise and NO_x, the observed low correlation points out to their different dispersion mechanisms.

This study showed that noise barriers could be used to reduce both noise and road-borne air pollution at receptor sides of barriers. For this reason, it is essential that noise barriers, frequently used in urban areas, are designed to simultaneously minimize the exposure of both noise and air pollutants at receptor points. Therefore, further studies are needed to optimize noise barrier designs with different physical or material properties and application scenarios.

CRediT authorship contribution statement

Melike Nese Tezel-Oguz: Conceptualization, Software utilization, Writing - original draft, Writing - review & editing, Visualization. Muhammed Marasli: Study site resources, Supervision. Deniz Sari: Methodology, Data curation. Nesimi Ozkurt: Investigation, Project administration. S. Sinan Keskin: Validation, Formal analysis, Funding acquisition.

Data availability

The data that has been used is confidential.

Declaration of competing interest

The authors declare the following financial interests/personal relationships which may be considered as potential competing interests: Melike Nese Tezel-Oguz reports financial support was provided by The Scientific and Technological Research Council of Turkiye.

Acknowledgments

This study was supported by the Scientific and Technological Research Council of Turkiye [Project number: 122Y248]. This study was performed with the support of Fibrobeton Inc., Republic of Turkiye Ministry of Environment, Urbanization, and Climate Change, in collaboration with TÜBİTAK Marmara Research Center (MAM). The authors thank for their considerable support and assistance before, during, and after the setup and monitoring period of the study to Volkan Özdal, Sefa Güntepe, Faik Ali Birinci (Fibrobeton Inc.); Soner Olgun, Onur Kale, Zekai Karaca (Ministry of Environment, Urbanization, and Climate Change); Fatma Pınar Aksoy-Kaya (TÜBİTAK MAM Air Quality and Environmental Noise Technologies Research Group).

References

Adair, D., Jaeger, M., 2014. Evaluation of model for air pollution in the vicinity of roadside solid barriers. Energy Environ. Eng. 2 (7), 145–152. https://doi.org/10.13189/eee.2014.020702.

Ahangar, F.E., Heist, D., Perry, S., Venkatram, A., 2017. Reduction of air pollution levels downwind of a road with an upwind noise barrier. Atmos. Environ. 155, 1–10. https://doi.org/10.1016/j.atmosenv.2017.02.001.

Amini, S., Ahangar, F.E., Schulte, N., Venkatram, A., 2016. Using models to interpret the impact of roadside barriers on near-road air quality. Atmos. Environ. 138, 55–64. https://doi.org/10.1016/j.atmosenv.2016.05.001.

Amini, S., Ahangar, F.E., Heist, D.K., Perry, S.G., Venkatram, A., 2018. Modeling dispersion of emissions from depressed roadways. Atmos. Environ. 186, 189–197. https://doi.org/10.1016/j.atmosenv.2018.04.058.

Baldauf, R., Thoma, E., Khlystov, A., Isakov, V., Bowker, G., Long, T., Snow, R., 2008. Impacts of noise barriers on near-road air quality. Atmos. Environ. 42 (32), 7502–7507. https://doi.org/10.3390/environments501000110.1016/j.atmosenv.2008.05.051.

Basner, M., Babisch, W., Davis, A., Brink, M., Clark, C., Janssen, S., Stansfeld, S., 2014. Auditory and non-auditory effects of noise on health. Lancet 383 (9925), 1325–1332. https://doi.org/10.1016/S0140-6736(13)61613-X.

Batterman, S., Ganguly, R., Harbin, P., 2015. High resolution spatial and temporal mapping of traffic-related air pollutants. Int. J. Environ. Res. Public Health 12 (4), 3646–3666. https://doi.org/10.3390/ijerph120403646.

Benson, P.E., 1992. A review of the development and application of the CALINE3 and 4 models. Atmos. Environ. B, Urban Atmos. 26 (3), 379–390. https://doi.org/10.1016/0957-1272(92)90013-I.

Borelli, D., Repetto, S., Schenone, C., 2014. Noise mapping of the flyover highway in Genoa: comparison of different methods. Noise Mapping 1 (1). https://doi.org/10.2478/noise-2014-0007.

Brook, R.D., Rajagopalan, S., Pope 3rd, C.A., Brook, J.R., Bhatnagar, A., Diez-Roux, A.V., ... Kaufman, J.D., 2010. Particulate matter air pollution and cardiovascular disease: an update to the scientific statement from the American Heart Association. Circulation 121 (21), 2331–2378. https://doi.org/10.1161/CIR.0b013e3181dbece1.

Cannelli, G.B., Gluck, K., Santoboni, S., 1983. A mathematical-model for evaluation and prediction of the mean energy-level of traffic noise in Italian towns. Acustica 53 (1), 31–36.

Cassina, L., Fredianelli, L., Menichini, I., Chiari, C., Licitra, G., 2018. Audio-visual preferences and tranquillity ratings in urban areas. Environments 5 (1), 17. https://doi.org/10.3390/environments5010001.

Coates, J., Mar, K.A., Ojha, N., Butler, T.M., 2016. The influence of temperature on ozone production under varying NOx conditions – a modelling study. Atmos. Chem. Phys. 16 (18), 11601–11615. https://doi.org/10.5194/acp-16-11601-2016.

Cooper, D.C., Alley, F.C., 2011. Air Pollution Control. 4 ed. Waveland Press Inc., United States of America.

CoRTN, 1988. Calculation of Road Traffic Noise. United Kingdom Department of Environment and welsh Office Joint Publication, HMSO 15.04.2016. URL: http://bailey.persona-pi.com/Public-Inquiries/M4-Newport/C%20-%20Core%20Documents/14.%20Noise%20and%20Vibration/14.2.1%20-%20Department%20of%20Transport%20and%20Welsh%20Office%20Calculation%20of%20Road%20Traffic%20Noise.%201988.pdf.

Danciulescu, V., Bucur, E., Pascu, L.F., Vasile, A., Bratu, M., 2015. Correlations between noise level and pollutants concentration in order to assess the level of air pollution induced by heavy traffic. J. Environ. Prot. Ecol. 16 (3), 815–823.

Davies, H.W., Vlaanderen, J.J., Henderson, S.B., Brauer, M., 2009. Correlation between co-exposures to noise and air pollution from traffic sources. Occup. Environ. Med. 66 (5), 347–350. https://doi.org/10.1136/oem.2008.041764.

Dekoninck, L., Severijnen, M., 2022. Correlating traffic data, spectral noise and air pollution measurements: retrospective analysis of simultaneous measurements near a highway in the Netherlands. Atmosphere 13 (5), 740. https://doi.org/10.3390/atmos13050740.

Ece, M., Tosun, İ., Ekinci, K., Yalçındağ, N.S., 2018. Modeling of road traffic noise and traffic flow measures to reduce noise exposure in Antalya metropolitan municipality. J. Environ. Health Sci. Eng. 16 (1), 1–10. https://doi.org/10.1007/s40201-018-0288-4.

EEA, 2020. Environmental Noise in Europe — European Environment Agency 2020 EEA Report No 22/2019. Publications Office of the European Union 28.01.2022 https://www.eea.europa.eu/publications/environmental-noise-in-europe.

EMEP/EEA, 2020. Air Pollutant Emission Inventory Guidebook 2019. European Environment Agency 10.10.2021 http://www.eea.europa.eu/publications/emep-eea-guidebook-2019/part-b-sectoral-guidance-chapters/1-energy/1-a-combustion/1-a-3-b-i.

END, 2002. Environmental Noise Directive 2002/49/EC - Relating to the Assessment and Management of Environmental Noise *189/12*. The European Parliament and of the Council 20.03.2017 https://publications.europa.eu/en/publication-detail/-/publication/27d1a64e-08f0-4665-a258-96f16c7af072/language-en.

Finn, D., Clawson, K.L., Carter, R.G., Rich, J.D., Eckman, R.M., Perry, S.G., ... Heist, D.K., 2010. Tracer studies to characterize the effects of roadside noise barriers on near-road pollutant dispersion under varying atmospheric stability conditions. Atmos. Environ. 44 (2), 204–214. https://doi.org/10.1016/j.atmosenv.2009.10.012.

Fiorini, C.V., 2022. Railway noise in urban areas: assessment and prediction on infrastructure improvement combined with settlement development and regeneration in Central Italy. Appl. Acoust. 185, 108413. https://doi.org/10.1016/j.apacoust.2021.108413.

Foraster, M., Deltell, A., Basagana, X., Medina-Ramon, M., Aguilera, I., Bouso, L., ... Kunzli, N., 2011. Local determinants of road traffic noise levels versus determinants of air pollution levels in a Mediterranean city. Environ. Res. 111 (1), 177–183. https://doi.org/10.1016/j.envres.2010.10.013.

Fuks, K.B., Weinmayr, G., Basagana, X., Gruzieva, O., Hampel, R., Oftedal, B., ... Hoffmann, B., 2017. Long-term exposure to ambient air pollution and traffic noise and incident hypertension in seven cohorts of the European study of cohorts for air pollution effects (ESCAPE). Eur. Heart J. 38 (13), 983–990. https://doi.org/10.1093/eurheartj/ehw413.

Ghasemian, M., Amini, S., Princevac, M., 2017. The influence of roadside solid and vegetation barriers on near-road air quality. Atmos. Environ. 170, 108–117. https://doi.org/10.1016/j.atmosenv.2017.09.028.

Gong, L., Wang, X., 2018. Numerical study of noise Barriers' side edge effects on pollutant dispersion near roadside under various thermal stability conditions. Fluids 3 (4), 105.

Hagler, G.S.W., Tang, W., Freeman, M.J., Heist, D.K., Perry, S.G., Vette, A.F., 2011. Model evaluation of roadside barrier impact on near-road air pollution. Atmos. Environ. 45 (15), 2522–2530. https://doi.org/10.1016/j.atmosenv.2011.02.030.

Hagler, G.S.W., Lin, M.-Y., Khlystov, A., Baldauf, R.W., Isakov, V., Faircloth, J., Jackson, L.E., 2012. Field investigation of roadside vegetative and structural barrier impact on near-road ultrafine particle concentrations under a variety of wind conditions. Sci. Total Environ. 419, 7–15. https://doi.org/10.1016/j.scitotenv.2011.12.002.

Hasmaden, F., Zorer Gedik, G., Yüğrük Akdağ, N., 2022. An approach to the design of photovoltaic noise barriers and a case study from Istanbul, Turkey. Environ. Sci. Pollut. Res. 29 (22), 33609–33626. https://doi.org/10.1007/s11356-022-18625-0.

HEI, 2010. Traffic-related Air Pollution: A Critical Review of the Literature on Emissions, Exposure, and Health Effects. Health Effects Institute Special Report 17. URL: https://www.healtheffects.org/system/files/SR17TrafficReview.pdf.

Heist, D.K., Perry, S.G., Brixey, L.A., 2009. A wind tunnel study of the effect of roadway configurations on the dispersion of traffic-related pollution. Atmos. Environ. 43 (32), 5101–5111. https://doi.org/10.1016/j.atmosenv.2009.06.034.

Heist, D., Isakov, V., Perry, S., Snyder, M., Venkatram, A., Hood, C., ... Owen, R.C., 2013. Estimating near-road pollutant dispersion: A model inter-comparison. Transp. Res. Part D: Transp. Environ. 25, 93–105. https://doi.org/10.1016/j.trd.2013.09.003.

Hooghwerff, J., Tollenaar, C.C., van der Heijden, W.J., 2010. In-situ air quality measurements on existing and innovative noise barriers. Air Pollution Xviii 136, 129–139. https://doi.org/10.2495/air100121.

Huertas, J.I., Aguirre, J.E., Lopez Mejia, O.D., Lopez, C.H., 2021. Design of road-side barriers to mitigate air pollution near roads. Appl. Sci. 11 (5). https://doi.org/10.3390/app11052391 Retrieved from.

IPCC, 2006. IPCC Guidelines for National Greenhouse Gas Inventories. MOBILE COMBUSTION 10.01.2016 http://www.ipcc-nggip.iges.or.jp/public/2006gl/.

Ising, H., Lange-Asschenfeldt, H., Moriske, H.J., Born, J., Eilts, M., 2004. Low frequency noise and stress: bronchitis and cortisol in children exposed chronically to traffic noise and exhaust fumes. Noise Health 6 (23), 21–28 doi: https://www.noiseandhealth.org/article.asp?issn=1463-1741;year=2004;volume=6;issue=23;spage=21;epage=28;aulast=Ising.

Jeong, S.J., 2015. A CFD study of roadside barrier impact on the dispersion of road air pollution. Asian J. Atmos. Environ. 9 (1). https://doi.org/10.5572/ajae.2015.9.1.022.

Kanda, I., Yamao, Y., Uehara, K., Ohara, T., 2011. A wind-tunnel study on diffusion from urban major roads. J. Wind Eng. Ind. Aerodyn. 99 (12), 1227–1242. https://doi.org/10.1016/j.jweia.2011.10.009.

Karantonis, P., Gowen, T., Simon, M., 2010. Further comparison of traffic noise predictions using the CadnaA and SoundPLAN noise prediction models. Paper presented at the Proceedings of 20th International Congress on Acoustics, ICA.

Kephalopoulos, S., Paviotti, M., Anfosso-Lédée, F., Van Maercke, D., Shilton, S., Jones, N., 2014. Advances in the development of common noise assessment methods in Europe: the CNOSSOS-EU framework for strategic environmental noise mapping. Sci. Total Environ. 482-483, 400–410. https://doi.org/10.1016/j.scitotenv.2014.02.031.

Khan, J., Ketzel, M., Kakosimos, K., Sørensen, M., Jensen, S.S., 2018. Road traffic air and noise pollution exposure assessment – a review of tools and techniques. Sci. Total Environ. 634, 661–676. https://doi.org/10.1016/j.scitotenv.2018.03.374.

Kheirbek, I., Ito, K., Neitzel, R., Kim, J., Johnson, S., Ross, Z., ... Matte, T., 2014. Spatial variation in environmental noise and air pollution in New York City. J. Urban Health 91 (3), 415–431. https://doi.org/10.1007/s11524-013-9857-0.

Kim, K.H., Ho, D.X., Brown, R.J.C., Oh, J.M., Park, C.G., Ryu, I.C., 2012. Some insights into the relationship between urban air pollution and noise levels. Sci. Total Environ. 424, 271–279. https://doi.org/10.1016/j.scitotenv.2012.02.066.

Klaeboe, R., Kolbenstvedt, M., Clench-Aas, J., Bartonova, A., 2000. Oslo traffic study - part 1: an integrated approach to assess the combined effects of noise and air pollution on annoyance. Atmos. Environ. 34 (27), 4727–4736. https://doi.org/10.1016/S1352-2310(00)00304-6.

Lee, E.S., Ranasinghe, D.R., Ahangar, F.E., Amini, S., Mara, S., Choi, W., ... Zhu, Y., 2018. Field evaluation of vegetation and noise barriers for mitigation of near-freeway air pollution under variable wind conditions. Atmos. Environ. 175, 92–99. https://doi.org/10.1016/j.atmosenv.2017.11.060.

Lercher, P., Evans, G.W., Meis, M., 2003. Ambient noise and cognitive processes among primary schoolchildren. Environ. Behav. 35 (6), 725–735. https://doi.org/10.1177/0013916503256260.

Medeiros, A.F.D. d, Pimentel, R.L., Melo, R.A.d., Araújo, B.C.D. d, Brasileiro, T.d.C., 2022. Investigation of traffic noise attenuation potential of an urban highway underpass. Appl. Acoust. 192, 108682. https://doi.org/10.1016/j.apacoust.2022.108682.

Mehta, D., Hazarika, N., Srivastava, A., 2020. Diurnal variation of BTEX at road traffic intersection points in Delhi, India: source, ozone formation potential, and health risk assessment. Environ. Sci. Pollut. Res. 27 (10), 11093–11104. https://doi.org/10.1007/s11356-019-07495-8.

Miedema, H.M.E., Oudshoorn, C.G.M., 2001. Annoyance from transportation noise: relationships with exposure metrics DNL and DENL and their confidence intervals. Environ. Health Perspect. 109 (4), 409–416. https://doi.org/10.2307/3454901.

Milford, I., Aasebo, S.J., Strommer, K., 2012. Value for money in road traffic noise abatement. Procedia Soc. Behav. Sci. 48, 1366–1374. https://doi.org/10.1016/j.sbspro.2012.06.1112.

Mioduszewski, P., Ejsmont, J.A., Grabowski, J., Karpiński, D., 2011. Noise map validation by continuous noise monitoring. Appl. Acoust. 72 (8), 582–589. https://doi.org/10.1016/j.apacoust.2011.01.012.

MoEUCC, 2022. Environmental Noise Control Regulation (Çevresel Gürültü Kontrol Yönetmeliği). Ministry of Environment, Urbanization and Climate Change, Republic of Turkiye 18.05.2023 https://www.resmigazete.gov.tr/eskiler/2022/11/20221130-1.htm.

Morakinyo, T.E., Lam, Y.F., 2016. Simulation study of dispersion and removal of particulate matter from traffic by road-side vegetation barrier. Environ. Sci. Pollut. Res. 23 (7), 6709–6722. https://doi.org/10.1007/s11356-015-5839-y.

NASA, 2021. Shuttle Radar Topography Mission (SRTM) 90 m Digital Elevation Data. 28.04.2021 https://earthexplorer.usgs.gov/.

Nast, D., Speer, W., Le Prell, C., 2014. Sound level measurements using smartphone "apps": useful or inaccurate? Noise Health 16 (72), 251–256. https://doi.org/10.4103/1463-1741.140495.

Ning, Z., Hudda, N., Daher, N., Kam, W., Herner, J., Kozawa, K., ... Sioutas, C., 2010. Impact of roadside noise barriers on particle size distributions and pollutants concentrations near freeways. Atmos. Environ. 44 (26), 3118–3127. https://doi.org/10.1016/j.atmosenv.2010.05.033.

NMPB. (1996). NMPB-Routes-96 (SETRA-CERTU-LCPC,CSTB), New french calculation method including meteorological effects.

NOAA, 2022. Pasquill Stability Classes. National Oceanic and Atmospheric Administration Air Resources Laboratory 07.04.2023 https://www.ready.noaa.gov/READYpgclass.php.

Pachón, J.E., Saavedra, C., Pérez, M.P., Galvis, B.R., Arunachalam, S., 2016. Exposure assessment to high-traffic corridors in Bogota using a near-road air quality model. Paper Presented at the Air Pollution Modeling and its Application XXIV, Cham.

Patterson, R.F., Harley, R.A., 2019. Evaluating near-roadway concentrations of diesel-related air pollution using RLINE. Atmos. Environ. 199, 244–251. https://doi.org/10.1016/j.atmosenv.2018.11.016.

Ranasinghe, D., Lee, E.S., Zhu, Y., Frausto-Vicencio, I., Choi, W., Sun, W., ... Paulson, S.E., 2019. Effectiveness of vegetation and sound wall-vegetation combination barriers on pollution dispersion from freeways under early morning conditions. Sci. Total Environ. 658, 1549–1558. https://doi.org/10.1016/j.scitotenv.2018.12.159.

Rao, X.Q., Zhong, J.X., Maiseyeu, A., Gopalakrishnan, B., Villamena, F.A., Chen, L.C., ... Rajagopalan, S., 2014. CD36-dependent 7-ketocholesterol accumulation in macrophages mediates progression of atherosclerosis in response to chronic air pollution exposure. Circ. Res. 115 (9), 770–U766. https://doi.org/10.1161/circresaha.115.304666.

Reiminger, N., Jurado, X., Vazquez, J., Wemmert, C., Blond, N., Dufresne, M., Wertel, J., 2020. Effects of wind speed and atmospheric stability on the air pollution reduction rate induced by noise barriers. J. Wind Eng. Ind. Aerodyn. 200, 104160. https://doi.org/10.1016/j.jweia.2020.104160.

RLS-90, 1990. Richtlinien für den Lärmschutz an Strassen. BM für Verkehr, Bonn 15.04.2016 https://www.gesund-am-stienitzsee.de/wp-content/uploads/RLS90-opt..pdf.

Ross, Z., Kheirbek, I., Clougherty, J.E., Ito, K., Matte, T., Markowitz, S., Eisl, H., 2011. Noise, air pollutants and traffic: continuous measurement and correlation at a high-traffic

location in New York City. Environ. Res. 111 (8), 1054–1063. https://doi.org/10.1016/j.envres.2011.09.004.
Schulte, N., Snyder, M., Isakov, V., Heist, D., Venkatram, A., 2014. Effects of solid barriers on dispersion of roadway emissions. Atmos. Environ. 97, 286–295. https://doi.org/10.1016/j.atmosenv.2014.08.026.
Shahidan, S., Hannan, N., Maarof, M.Z.M., Leman, A.S., Senin, M.S., 2017. A comprehensive review on the effectiveness of existing noise barriers commonly used in the railway industry. Paper Presented at the 9th International Unimas Stem Engineering Conference, Cedex A ://WOS:000390796100007.
Shu, S., Yang, P., Zhu, Y., 2014. Correlation of noise levels and particulate matter concentrations near two major freeways in Los Angeles, California. Environ. Pollut. 193, 130–137. https://doi.org/10.1016/j.envpol.2014.06.025.
Sillman, S., 2003. Tropospheric ozone and photochemical smog. (1 ed., Chapter 9.11, pp. 407-431)In: Lollar, B.S. (Ed.), Treatise on Geochemistry, 1 ed. Elsevier.
Snyder, M.G., Venkatram, A., Heist, D.K., Perry, S.G., Petersen, W.B., Isakov, V., 2013. RLINE: a line source dispersion model for near-surface releases. Atmos. Environ. 77, 748–756. https://doi.org/10.1016/j.atmosenv.2013.05.074.
SoundPLAN, 2019. SoundPLAN User's Manuel. SoundPLAN GmbH / SoundPLAN International LLC.
Steffens, J.T., Wang, Y.J., Zhang, K.M., 2012. Exploration of effects of a vegetation barrier on particle size distributions in a near-road environment. Atmos. Environ. 50, 120–128. https://doi.org/10.1016/j.atmosenv.2011.12.051.
Steffens, J.T., Heist, D.K., Perry, S.G., Zhang, K.M., 2013. Modeling the effects of a solid barrier on pollutant dispersion under various atmospheric stability conditions. Atmos. Environ. 69, 76–85. https://doi.org/10.1016/j.atmosenv.2012.11.051.
Steffens, J.T., Heist, D.K., Perry, S.G., Isakov, V., Baldauf, R.W., Zhang, K.M., 2014. Effects of roadway configurations on near-road air quality and the implications on roadway designs. Atmos. Environ. 94, 74–85. https://doi.org/10.1016/j.atmosenv.2014.05.015.
Sygna, K., Aasvang, G.M., Aamodt, G., Oftedal, B., Krog, N.H., 2014. Road traffic noise, sleep and mental health. Environ. Res. 131, 17–24. https://doi.org/10.1016/j.envres.2014.02.010.
Tang, U.W., Wang, Z.S., 2007. Influences of urban forms on traffic-induced noise and air pollution: results from a modelling system. Environ. Model. Softw. 22 (12), 1750–1764. https://doi.org/10.1016/j.envsoft.2007.02.003.
Thiruvenkatachari, R.R., Ding, Y., Pankratz, D., Venkatram, A., 2022. A field study to estimate the impact of noise barriers on mitigation of near road air pollution. Air Qual. Atmos. Health 15 (2), 363–372. https://doi.org/10.1007/s11869-021-01104-9.
Tong, Z., Baldauf, R.W., Isakov, V., Deshmukh, P., Max Zhang, K., 2016. Roadside vegetation barrier designs to mitigate near-road air pollution impacts. Sci. Total Environ. 541, 920–927. https://doi.org/10.1016/j.scitotenv.2015.09.067.
Tsai, K.T., Lin, M.D., Lin, Y.H., 2019. Noise exposure assessment and prevention around high-speed rail. Int. J. Environ. Sci. Technol. 16 (8), 4833–4842. https://doi.org/10.1007/s13762-018-2047-6.
TURKSTAT, 2021. Road Motor Vehicle Statistics, Number of Motor Vehicles by Type of Fuel Used. Turkish Statistical Institue (Türk Standartları Enstitüsü).
USDT, 2010. Highway Traffic Noise: Analysis and Abatement Guidance. 01.01.2016 https://www.fhwa.dot.gov/environment/noise/regulations_and_guidance/analysis_and_abatement_guidance/revguidance.pdf.
USEPA, 1992. Protocol for Determining the Best Performing Model. Publication No. EPA-454/R-92-025. U. S. E. P. Agency. https://www.epa.gov/sites/default/files/2020-10/documents/model_eval_protocol.pdf.
USEPA, 2007. Emissions Factors & AP 42. Technology Transfer Network Clearinghouse for Inventories & Emissions Factors. United States Environmental Protection Agency 15.01.2016 https://www.nrc.gov/docs/ML0907/ML090770907.pdf.
USEPA, 2021. Trends in Ozone Adjusted for Weather Conditions. United States Environmental Protection Agency 23.04.2023 https://19january2021snapshot.epa.gov/air-trends/trends-ozone-adjusted-weather-conditions_.html#:~:text=Ozone%20is%20more%20readily%20formed,cool%2C%20rainy%2C%20or%20windy.
USEPA, 2022. Nitrogen Oxides (NOx) Control Regulations. 20.01.2022 https://www3.epa.gov/region1/airquality/nox.html.
Venkatram, A., Schulte, N., 2018. Chapter four - the impact of highways on urban air quality. In: Venkatram, A., Schulte, N. (Eds.), Urban Transportation and Air Pollution. Elsevier , pp. 77–104. https://www.sciencedirect.com/science/article/pii/B978012811506000004X.
Venkatram, A., Isakov, V., Deshmukh, P., Baldauf, R., 2016. Modeling the impact of solid noise barriers on near road air quality. Atmos. Environ. 141, 462–469. https://doi.org/10.1016/j.atmosenv.2016.07.005.
Venkatram, A., Heist, D.K., Perry, S.G., Brouwer, L., 2021. Dispersion at the edges of near road noise barriers. Atmos. Pollut. Res. 12 (2), 367–374. https://doi.org/10.1016/j.apr.2020.11.017.
Wang, S., Wang, X., 2021. Modeling and analysis of highway emission dispersion due to noise barrier and automobile wake effects. Atmos. Pollut. Res. 12 (1), 67–75. https://doi.org/10.1016/j.apr.2020.08.013.
Wang, Y., Guo, H., Zou, S., Lyu, X., Ling, Z., Cheng, H., Zeren, Y., 2018. Surface O3 photochemistry over the South China Sea: application of a near-explicit chemical mechanism box model. Environ. Pollut. 234, 155–166. https://doi.org/10.1016/j.envpol.2017.11.001.
Xu, C., He, X., Sun, S., Bo, Y., Cui, Z., Zhang, Z., Dong, H., 2022. Sensitivity of ozone formation in summer in Jinan using observation-based model. Atmosphere 13 (12), 2024. https://doi.org/10.3390/atmos13122024.
Zannetti, P., 2013. Air Pollution Modeling: Theories, Computational Methods and Available Software. Springer Science & Business Media.
Zannin, P.H.T., do Nascimento, E.O., da Paz, E.C., do Valle, F., 2018. Application of artificial neural networks for noise barrier optimization. Environments 5 (12). https://doi.org/10.3390/environments5120135.
Zhai, X., Russell, A.G., Sampath, P., Mulholland, J.A., Kim, B.-U., Kim, Y., D'Onofrio, D., 2016. Calibrating R-LINE model results with observational data to develop annual mobile source air pollutant fields at fine spatial resolution: application in Atlanta. Atmos. Environ. 147, 446–457. https://doi.org/10.1016/j.atmosenv.2016.10.015.